Summer 7-2015

Antioxidant Mechanisms of Glutathione against Metal-Mediated Oxidative DNA Damage

Elias Eteshola
Rose-Hulman Institute of Technology, eteshoe@rose-hulman.edu

Antioxidant Mechanisms of Glutathione against Metal-Mediated Oxidative DNA Damage

A Thesis

Submitted to the Faculty

of

Rose-Hulman Institute of Technology

by

Elias Eteshola

In Partial Fulfillment of the Requirements for the Degree

of

Master of Science in Chemistry

July 2015

ROSE-HULMAN INSTITUTE OF TECHNOLOGY

Final Examination Report

Elias Eteshola — Name

Chemistry — Graduate Major

Thesis Title: Antioxidant Mechanisms of Glutathione Against Metal-Mediated Oxidative DNA Damage

DATE OF EXAM: July 10, 2015

EXAMINATION COMMITTEE:

	Thesis Advisory Committee	Department
Thesis Advisor:	Daniel Morris	CHEM
	Ross Weatherman	CHEM
	Adam Nolte	CHE

PASSED X **FAILED** _____

ABSTRACT

Eteshola, Elias

M.S.CHEM

Rose-Hulman Institute of Technology

July 2015

Antioxidant Mechanisms of Glutathione against Metal-Mediated Oxidative DNA Damage: A Comprehensive Study

Thesis Advisor: Dr. Daniel L. Morris, Jr.

Oxidative damage of DNA strands has been strongly linked with the development of diseases such as certain cancers, cystic fibrosis and Parkinson's, as well as aging. In intercellular reactions involving hydrogen peroxide endogenous metals have been shown to increase the generation of site-specific base modifications through their formation of reactive oxygen species (ROS). The damage markers measured via HPLC are the 8-hydroxy-2'-deoxyguanosine (8-OH-dG) and the dA-*N*1 oxide markers. The current study deals with the reduced form of the sulfur antioxidant glutathione (GSH) and elucidating its ameliorating effects against ROS formation. Comparative studies with the known radical-scavenging sulfur antioxidant dimethyl sulfoxide (DMSO) have also been performed. The fluorescent probe 2',7'-dichlorofluorescein (DCF) was used to quantify the ROS production both in the presence and absence of both GSH and DMSO. Metal binding studies were conducted using isothermal titration calorimetry (ITC) in order to better interrogate the nature of the metal ion interactions with GSH. A better understanding of antioxidant mechanisms against oxidative DNA damage will eventually lead to the development of better therapeutics and treatment options against the aforementioned ailments and conditions in the future.

DEDICATION

I would like to dedicate this thesis to my parents, brothers, and sister who continued to push me to strive for excellence in all facets of my life. My parents, Edward and Lois Eteshola, have proved me with years of love, care, and support as well as instilled in me the importance of setting a good example for my younger siblings. Thanks to your amazing parenting, constant support and countless hours of prayer, I have completed another major step in my academic training. Thank you very much! I love you both dearly!

ACKNOWLEDGEMENTS

The culmination of this thesis has been only possible thanks to the assistance, support, and guidance of several people including my thesis advisor Dr. Daniel Morris, Jr. and Rose-Hulman Institute of Technology Chemistry & Biochemistry Department Lab Manager Lou Johnson. I would also like to thank the Department Stockroom Manager, Cyndi Erwin. I am also very appreciative of the other members of my thesis committee, Drs. Weatherman and Nolte. I also am very grateful to Lee Anne Siemer who was always patient when it came to answering lab questions and was kind enough to share her GSH damage marker study data which helped in developing Figures 3 and 5. Of course my family and friends are much appreciated for all the encouragement and support they provided along this journey. Finally, I must give thanks to God who blessed me with the strength to keep preserving throughout my whole time at Rose-Hulman.

TABLE OF CONTENTS

Contents

LIST OF FIGURES

Figure **Page**

LIST OF TABLES

Table **Page**

LIST OF ABBREVIATIONS

8-OH-dG	**8-hydroxy**-2'-**d**eoxy**g**uanosine
A	**A**denine
AP-1	**A**ctivator **P**rotein transcription factor
ARE	**A**ntioxidant **R**esponsive **E**lement
C	**C**ytosine
dA	2'-**d**eoxy**a**denosine
dA *N*-1 oxide	2'-**d**eoxy**a**denosine ***N*-1 oxide**
dC	2'-**d**eoxy**c**ytidine
DCF	2',7'-**dic**hloro**f**luorescein
DCF-DA	**D**ihydrodi**c**hloro**f**luorescein **di**a**c**etate
dG	2'-**d**eoxy**g**uanosine
DMSO	**D**i**m**ethyl **s**ulf**o**xide
DNA	**D**eoxyribo**n**ucleic **a**cid
DSB	**D**ouble **S**trand **B**reak
dT	2'-**d**eoxy**t**hymidine
EPR	**E**lectron **P**aramagnetic **R**esonance spectroscopy
ESR	**E**lectron **S**pin **R**esonance spectroscopy
G	**G**uanine
GPx	**G**lutathione **p**ero**x**idase
GSH	**G**luta**thione** (reduced form)

GSSG	**G**luta**thione disulfide** (oxidized form)
HNE	4-**h**ydroxy**n**on**e**nal
HPLC	**H**igh **P**ressure/**P**erformance **L**iquid **C**hromatography
HR	**H**igh-**R**esolution
HT-FID	**H**igh-**t**hroughput **F**luorescent **I**ntercalator **D**isplacement assay
ITC	**I**sothermal **T**itration **C**alorimetry
MDA	**M**alon**dia**ldehyde
MS	**M**ass **S**pectrometry
MULTIS	spin trapping-based **Multi**ple Free-Radical **S**cavenging
NaAsc	**Sodium asc**orbate
NADH	**N**icotinamide **a**denine **d**inucleotide (**reduced** form)
NF-κB	**N**uclear **F**actor **kappa**-light-chain-enhancer of Activated **B** cells DNA transcription protein complex
ODS	**O**cta**d**ecyl**s**ilane
RNA	**R**ibo**n**ucleic **a**cid
RNS	**R**eactive **N**itrogen **S**pecies
ROS	**R**eactive **O**xygen **S**pecies
SOD	**S**uper**o**xide **d**ismutase
SSB	**S**ingle **S**trand **B**reak
T	**T**hymine
U	**U**racil
UV	**U**ltra**v**iolet

LIST OF SYMBOLS

English Symbols

J	joule
K	kelvin
mol	mole
M	Mole/liter (Molar)
W	watt

Mathematical Symbols

ΔG	Gibbs free energy
ΔH_o	Binding enthalpy
K_a	Binding affinity constant
n	Binding stoichiometry
R	Universal gas constant
ΔS_o	Binding entropy

1. INTRODUCTION

Deoxyribonucleic acid or DNA has often been called the driving force behind life. This double helical biomolecule contains all the necessary genetic information needed to pass from one generation to the next in all living organisms. While there are quite a few methods by which DNA can be damaged (oxidation, alkylation, and cross-linking), one of the most debilitating paths is oxidative damage via reactive oxygen species (ROS) which lead to single and double strand breaks (SSB and DSB) [1–2]. These ROS are oxygen-containing molecules such as hydroxyl radicals (·OH), superoxide ($\cdot O_2^-$) and peroxide ions (O_2^{2-}). These compounds are the natural byproducts of cellular respiration causing the oxidation of lipids, nucleic acids, and proteins [3]. While these ROS are actually very essential to many cellular processes such as cell signaling pathways and homeostasis [4], an imbalance in the endogenous ROS levels – such as under oxidative stress conditions – can lead to the generation of the strong oxidizing species that can damage lipids, membranes, and DNA. Damage to DNA – in the form of lesions, strand breaks, base modifications and DNA crosslinking – can interfere with cellular replication and transcription [5]. Interference with these vital processes can lead to chromosomal instability, a condition that has been implicated in many solid and hematological cancers [6], as well as other mutagenic changes to the host's DNA. Such changes force the host's cells to trigger apoptotic pathways (cell death) or lead to tumorigenesis [5].

Redox active endogenous metals such as iron and copper can readily generate the highly-reactive ROS. Amongst these various species is the formation of the most damaging radical species [7–8] – the hydroxyl radical (·OH) – via the reduction of hydrogen peroxide, a non-radical species derived from oxygen metabolism [9]. Metal-mediated ·OH is generated via the Fenton (iron metal

ion specific, *Reaction a*) or Fenton-like reactions [7, 9] for metals such as copper which are prone to redox cycling (*Reactions b–c*).

$$Fe^{II} + H_2O_2 \rightarrow Fe^{III} + {}^{-}OH + {}^{\cdot}OH \qquad \textbf{(a)}$$

$$Cu^{I} + H_2O_2 \rightarrow Cu^{II} + {}^{-}OH + {}^{\cdot}OH \qquad \textbf{(b)}$$

$$Cu^{II} \xrightarrow{red.} Cu^{I} + H_2O_2 \rightarrow Cu^{II} + {}^{-}OH + {}^{\cdot}OH \qquad \textbf{(c)}$$

Hydroxyl radical formation is catalytic in the presence of cellular reductants, such as NADH or ascorbic acid, which can reduce the oxidized metal ions back to their ·OH generating oxidation states [7]. Typically cells control the labile (non-protein bound) metal ion concentration [7], however, under oxidative stress conditions, iron and copper levels tend to increase to the point that the native cellular machinery cannot mitigate the harmful effects of the ROS buildup by the endogenous antioxidants available. These ROS may leak out of the mitochondria into the cytosol and hence into the rest of the cell [10]. In fact, it has been estimated that in normal cells 1–2% of oxygen molecules consumed by mitochondria end up as ROS [10]; these levels may increase by several orders of magnitude when the mitochondrion experiences oxidative stress.

Yet, other oxidants arise as by-products of various oxygen-utilizing enzymes, including those in peroxisomes (the cytoplasmic bodies that are involved in the oxidation of various cellular constituents, particularly lipids) [10]. The spontaneous oxidation of lipids results in lipid peroxidation (or the oxidative degradation of the aforementioned lipids). Since both eukaryotic and prokaryotic organisms utilize cell membranes composed of a selectively permeable lipid

bilayer [11], peroxidation would lead to the formation of reactive aldehydes, such as malondialdehyde (MDA) and 4-hydroxynonenal (HNE) [12–13]. These reactive intermediates are both mutagenic and carcinogenic. For example, MDA reacts with deoxyadenosine and deoxyguanosine (dA and dG respectively) to form DNA adducts, primarily M_1G [12].

The limited options for protection against physical carcinogens, such as ultraviolet (UV) rays and ionizing radiation from X-rays, contrast against the large number of mechanisms that cells employ in order to intercept chemical carcinogens (such as those found in pesticides and the polycyclic aromatic hydrocarbons found in tobacco smoke) before they can severely damage the cellular genome [10]. The sequestering of reactive oxygen species falls upon a class of compounds called antioxidants, which inhibit the oxidation of other molecule using a variety of mechanisms to prevent the radical chain reactions from propagating [14]. These compounds include a variety of enzymes, thiols, polyphenols (including superoxide dismutase (SOD), catalase, glutathione, and vitamin A), vitamin C (L-ascorbic acid), and vitamin E (α-tocopherol). Due to the fact that these compounds detoxify the effects of ROS by being oxidized themselves and leaving behind the unreactive forms of oxygen, these compounds often tend to be reducing agents [10, 14–15].

Insufficient levels of antioxidants or inhibition of the antioxidant molecule (or a mutation in the gene that encodes the enzyme) cause oxidative stress and may damage or kill cells [16–17]. Oxidative stress plays a significant role in many diseases. The use of antioxidants in pharmacology is intensively studied, particularly as treatments for strokes, Alzheimer's, Parkinson's, and other neurodegenerative diseases [18–22]. A comprehensive understanding of the mechanisms by which the various types of antioxidants alleviate the harmful effects of ROS will lead to a developmental breakthrough in the types of therapeutics that are available to combat many of the aforementioned ailments.

The purpose of this study is to provide a detailed and interrogative evaluation of the mechanism by which the reduced form of the sulfur-based antioxidant glutathione (GSH) functions. The overarching goal of this study aims at answering if GSH ameliorates the damaging effects of metal-initiated oxidative DNA damage via a radical scavenging scheme. This mechanism has been observed in some selenium antioxidants. The experiments also aim to examine if there are GSH-DNA adducts forming that blocks the sites of ROS attack on the DNA or if the preventative measure exhibited by this sulfur antioxidant involves metal coordination that inhibits the activation of hydrogen peroxide into the damaging hydroxyl radical. With this approach, the foundational groundwork concerning the operational parameters of these antioxidants can be laid. Future prospective studies could then be developed to optimize the effects of GSH and GSSG (the oxidized form of glutathione) against this type of DNA damage and could contribute to the development of therapies for cancer, inflammatory and neurodegenerative diseases.

Chapter 2 provides a comprehensive literature review of previous studies on selenium and sulfur antioxidants and the mechanisms by which they combat ROS *in vitro* and *in vivo* as well as a brief background and overview of current research relevant to the sulfur antioxidants of interest for this research. The literature mechanisms are described based on available antioxidant study results, experimental data and metal binding studies. This chapter includes a discussion of the various proposed mechanisms that are used in this thesis.

In Chapter 3, a description of the model system and the reasoning behind choosing this system is given. In addition, a brief overview and rationale of each of the experiments conducted is given. The exact experimental parameters, variables and measurements are given later in Chapter 4 of this thesis. Based on the current available data from previous work done by the Morris

Lab [8] in the area of antioxidant mechanisms as well as current work being done in the field, several experiments were designed to interrogate the model system and answer the GSH/DNA adduct or metal coordination hypothesis.

Chapter 4 gives a detailed account of the different materials and experimental methods used in this study. Specifically, the chapter will examine the reasoning behind why the experiments could be used to draw biologically relevant conclusions from the in vitro studies conducted that can be seen in Chapter 5. The results and accompanying figure(s) of each study as well as a statistical analysis of those said results are presented in Chapter 5. These outcomes help set the tone and the basis of the discussion that takes place in Chapter 6.

The discussion given in Chapter 6 helps in drawing experimental conclusions and establishing the directions that future studies could take for the presented model system and antioxidant analysis that are described in Chapter 7. Specifically, extensions of the metal coordination theory are discussed as well as improvements to the design parameters and variable control of the thermodynamic binding studies. Limitations, as well as possible redefined scopes of study are also presented in that chapter. In addition, a brief overview of alternative experiments and their theoretical expectations are also discussed.

2. BACKGROUND + LITERATURE REVIEW

One of the most studied reactions in free radical biology and chemistry is the Fenton reaction involving the oxidation of iron(II) to iron(III) by hydrogen peroxide to form a hydroxyl radical and hydroxide ions (·OH and $^{-}$OH respectively). This titular redox cycling reaction and its analogs (involving other redox active metals) was first observed by Henry John Horstman Fenton over 120 years ago [15, 23]. The broad reach of the Fenton reaction can be seen in its successful implementation in environmental engineering applications – such as wastewater treatment and groundwater remediation – and the fact that it has been implicated in various biological ailments including cancer and aging [23].

However, the Fenton reaction is not the only peculiar step in the oxidative DNA damage pathway. The ROS and the analogous reactive nitrogen species (RNS) have what has been commonly identified as a "two-face" nature [17, 24] since they are both beneficial and deleterious to biological systems. These ROS can act as secondary messenger molecules and activate intracellular signaling cascades, which have been associated with maintaining the oncogenic phenotype in tumor cells [24–26]. However, these reactive species can also induce cellular senescence and apoptosis and can, therefore, function as anti-tumorigenic species [24–26]. As mentioned in the previous chapter, a cellular redox imbalance and accompanying ROS buildup as a result of oxidative stress conditions can lead to the development of cellular hyperplasia and tumorigenesis [10, 26].

As mentioned previously, DNA is a very large, supercoiled biopolymer composed of nucleotide units and is usually found in the right-handed or B-DNA double helical form in cells [27]. The nucleotides are connected via phosphodiester linkages along the DNA chain, with the

complimentary nucleic bases on the two strands being joined via hydrogen bonding [27] within the interior of the polymer. Each nucleotide unit consists of a cyclic sugar (β-D-ribose in RNA or β-D-2' deoxyribose in DNA), which is phosphorylated at the 5' position. The sugar also has a heterocyclic nitrogenous base attached at the *C1'* position [28]. These heterocyclic bases consist of two main classes, the purines and the pyrimidines, which can be seen in Figure 1 below. The purine bases include the nucleotide bases guanine (G) and adenine (A) and are the most prevalent, naturally-occurring heterocycles in nature [28–29]. The pyrimidine nucleobases consist of cytosine (C) and thymine (T) in DNA or uracil (U) in RNA [28].

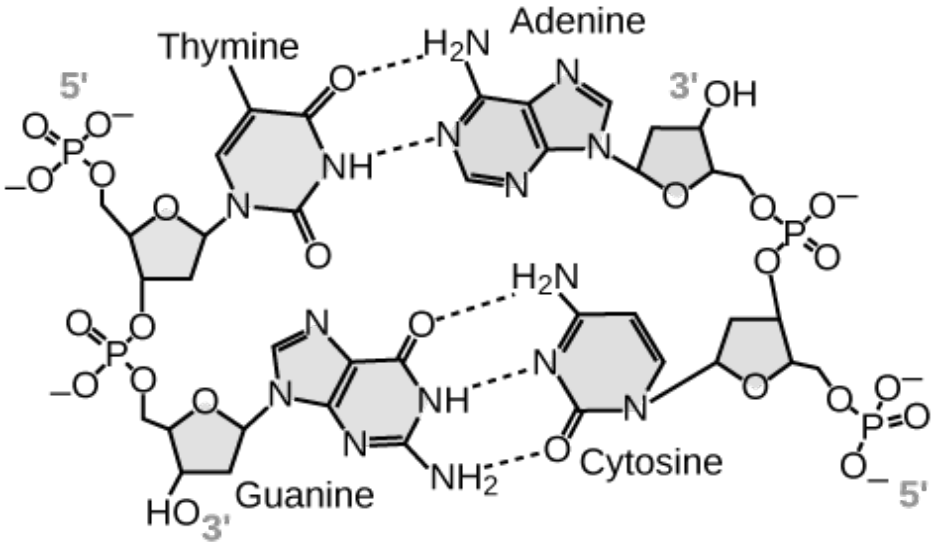

Figure 1. Heterocyclic nitrogenous bases that form the building blocks for the polymeric nucleic acids DNA and RNA. The structural differences between the two main classes of nitrogenous bases, the purines and pyrimidines, are shown. The purines include guanine (G) and adenine (A), which are larger heterocyclic systems than the pyrimidines and occur in both DNA and RNA. The pyrimidines include cytosine (C), thymine (T), and uracil (U). Uracil occurs naturally only in RNA, while thymine only occurs in DNA. Methylation of uracil leads to thymine. The figure also illustrates how the complimentary bases bind via hydrogen bonds. [30]

Due to their phosphate backbone, nucleic acids are polyanionic in nature, as can be seen in Figure 1, and tend to be negatively charged overall at physiological pH [28]. Such a charge distribution means that nucleic acids such as DNA require cations to provide charge stabilization [28]. This cationic source includes metal ions, protonated amines (such as spermine, putrescine, and spermidine), and protonated amino acid residues (such as histidine, arginine, and lysine) [28]. Alkali metal ions tend to provide partial charge neutralization by condensing around DNA in a cylindrical manner [31]. Yet, despite the various sources of positive charges with which DNA can interact, it still has a preferential affinity for cationic metal ions [27], especially transition metal ions. The degree of this interaction between these positively charged metal ions and the DNA depends on the electron density available at the exposed negatively charged regions of the DNA strands [27], such as the phosphate backbone or the nucleophilic atoms on the nitrogenous bases.

Metal ions can interact with DNA in a few ways. One method includes the metal directly coordinating to the DNA, usually at either the phosphate or sugar oxygen atoms, the nitrogenous base atoms, or a combination of all of these sites [27–28] as described by Anastassopoulou [27]. The most common sites of metal coordination in the nucleobases are the *N7*, *N1* and *O6* of the purines and the *N3* of pyrimidines [28]. In fact *N7* is particularly susceptible to alkylating agents and metal coordination due to its lone pair being sp^3 hybridized and not contributing to aromaticity or resonance of the purine, thus making it more nucleophilic and reactive [32]. The other interaction method is more indirect and can occur via other DNA ligands, including hydrogen bonding [28]. Transition metals have partially filled d-orbitals which means they can behave as free radicals and interact with more than one site on the DNA [27], making their interactions more complicated to study. Most of the transition metals react with the purine *N7* and pyrimidine *N3* atoms to perturb the double helical structure. Such perturbations can lead to various adducts and

lesions in the DNA, especially at the G–C sites in the DNA where the coordinated metal ions can generate free radicals through H_2O_2 oxidation [27].

One of the fundamental observations associated with many solid tumors, such as breast cancer, is the accumulation of DNA mutations in both the nuclear and mitochondrial DNA [17]. Such etiological mutations lead to chromosomal instability and oxidative DNA lesions that can be measured via the hydroxylated guanine derivative 8-hydroxy-2'-deoxyguanosine (8-OH-dG), a commonly accepted site-specific DNA damage marker [8, 17, 24]. The ROS can then activate the AP-1 (activator protein transcription factor) and NF-κB (nuclear factor kappa-light-chain-enhancer of activated B cells DNA transcription protein complex) signal transduction pathways that lead to the upregulation of the genes being transcribed in the cell proliferation and differentiation control pathways [33–36].

One of the most recognized radical-induced DNA damage markers is the 8-OH-dG (or 8-oxo-dG in its tautomeric form) lesion. Due to the high oxidation potential of the guanine base compared to those of cytosine, thymine, and adenine, it is readily oxidized to form the very mutagenic 8-OH-dG lesion [37–39]. The mutagenicity of 8-oxo-dG lesions is due to its miscoding propensity reflected in GC→TA transversion taking place during the DNA repair process [40]. Simply put, this non-naturally occurring nucleobase can incorrectly pair with both adenine and cytosine at the same efficiency as the normal guanine base [38–39, 41–42]. The deleterious consequence of such efficiency would lead to an alteration in the genetic information being transcribed from the DNA to the messenger RNA and consequently affect the RNA splicing, translation, and post-translational modification of the target protein being synthesized. Yet, DNA can also display the hallmarks of non-radical induced damage in the presence of a high cellular H_2O_2 concentration [43]. Such damage can be measured with the widely accepted non-radical

DNA damage marker 2'-deoxyadenosine *N*-1 oxide, or dA *N*-1 oxide, which occurs when 2'-deoxyadenosine (dA) is oxidized via an ionic pathway [8, 43].

Several techniques and assays have been developed to quantify and identify DNA damage in biological systems including the Ames test [10], the Comet assay (Single/Cell Gel Electrophoresis) [44], high-pressure liquid chromatography (HPLC) with a monoclonal anti-8-oxoG antibody [45], and HPLC-MS/MS [46]. It has been shown that HPLC combined with tandem mass spectrometry operating in mild electrospray mode is a very accurate and sensitive method of measuring oxidized nucleosides including 8-oxo-7,8-dihydro-2'-deoxyguanosine, 8-oxo-7,8-dihydro-2'-deoxyadenosine, 5-formyl-2′-deoxyuridine, 5-hydroxymethyl-2'-deoxyuridine, 5-hydroxy-2'-deoxyuridine, and the four diastereomers of 5,6-dihydroxy-5,6-dihydrothymidine within isolated and cellular DNA [46].

Just as redox active metals have been shown to help generate ROS, redox inactive metals such as cadmium (Cd), arsenic (As) and lead (Pb) show their lethal effects via bonding to sulfhydryl groups of proteins and depleting the cells cache of glutathione [15]. Zinc (Zn), a redox inert metal, is an essential component of numerous proteins involved in the defense against oxidative stress [15]. Thus the depletion of Zn may enhance DNA damage by inhibiting DNA repair mechanisms [15]. It has been shown that many low-molecular weight antioxidants, such as GSH, vitamins C and E, and carotenoids are capable of chelating metal ions and drastically reduce their catalytic ability to form ROS [14–15]. Some studies have been reported regarding the development of novel "dual-function" hybrid antioxidants that not only chelate metal ions but also have radical scavenging capabilities [47]. Such antioxidants would be very effective therapeutic options against diseases involving oxidative stress. Studies have looked into the use of polyphenols (due to their intrinsic reducing natures) as a means of activating endogenous biological defense

systems [48]. These compounds can achieve such results by stimulating antioxidant transcription and detoxification defense systems through antioxidant responsive elements (AREs) that are present in the promoter regions of many of the genes induced by oxidative and chemical stress [48].

Investigators have also used radical-induced hemolysis to determine the antioxidant capacity of novel compounds [49]. Yet, past work in this area has shown that this assay results in complete depletion of cellular GSH in biological systems [49]. Reduced glutathione (γ-L-Glutamyl-L-cysteinylglycine or GSH), as can be seen in Figure 2, is a cysteine-containing tripeptide with reducing and nucleophilic properties that play an important role in cellular protection from oxidative damage of lipids, proteins and nucleic acids [50]. The gamma peptide linkage in GSH is unique since it involves the amino group of the cysteine being bound to the *terminal* carboxylic acid of the glutamate side chain. This linkage is in contrast of the main alpha carboxyl group of the amino acid residue that would usually be involved in the case of a normal peptide bond. The advantage of this unique linkage is that it is resistant to degradation by all cellular enzymes except gamma-glutamyl transpeptidase (γ-GT) [51].

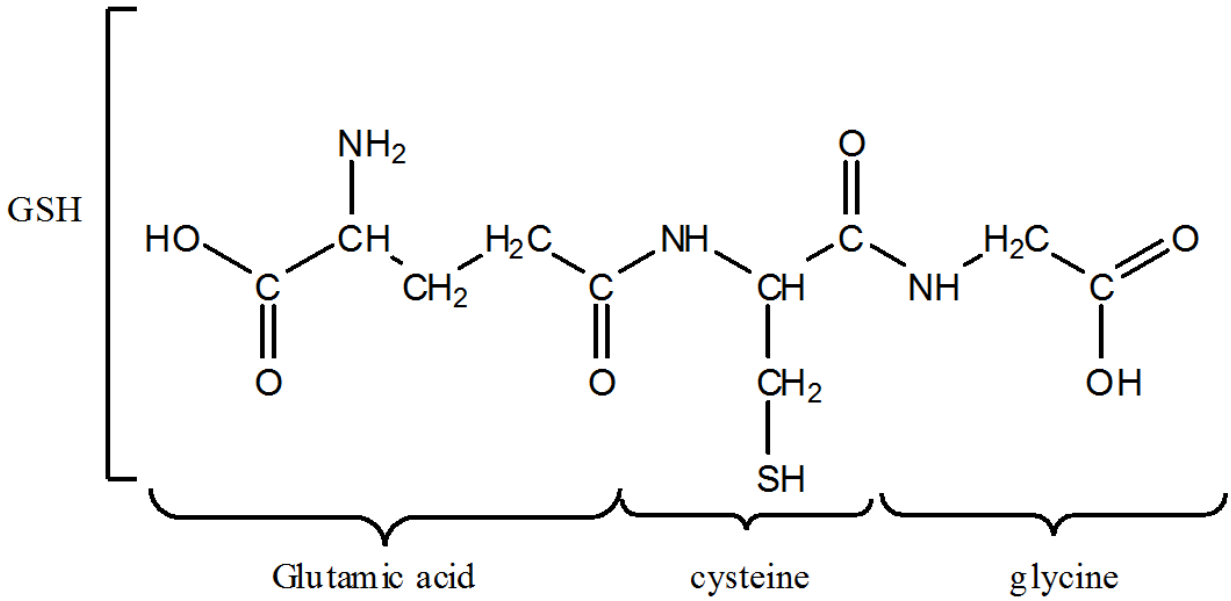

Figure 2. Basic component makeup of the reduced form of glutathione or GSH. This tripeptide antioxidant consists of a gamma peptide linkage between the carboxyl group of the glutamate side-chain and the amine group of the cysteine. The cysteine is then attached to the glycine by normal peptide linkage. [52]

Thus the work done by Jani et al. on radical-induced hemolysis demonstrates the addition of exogenous GSH necessary to make any useful antioxidant capacity measurements [49]. Other investigators have explored the novel use of a bioactive probe of the oxidative pentose phosphate cycle (OxPhos™ test) to quantify glutathione recycling dependent antioxidant activity in whole blood and intact human and rodent cells without the need for the isolation and cytoplasm extraction of cells [53]. Such advances can be used in pharmacological studies to screen drugs that improve the glutathione-dependent antioxidant capacity and not just the glutathione level since mammalian cells require glutathione dependent pathways for antioxidant activity [53]. Other applications of this test include quicker and more reliable detection methods for many oxidative stress related diseases including stroke and cardiovascular diseases and could be useful in detecting chemotherapeutic response and toxicity [53].

Previous studies into chalcogenic (of the *oxygen family*) antioxidants have shown that the protective effects of sulfur and selenium compounds is mainly achieved via radical scavenging and enzymatic decomposition metabolites using enzymes such as SOD and glutathione peroxidase (GPx) [3, 24, 54]. Previous work from Collins et al. have shown that some selenium–copper compounds are capable of utilizing both metal coordination and ROS scavenging [3, 55]. Work done by Hart et al. has explored the mechanisms by which selenium compounds such as selenium dioxide and selenite ion coordinate with metal ions (free and DNA-bound) [8].

In the present study, the metal ions Cu(II), Fe(II), and Cu(I) were allowed to react with H_2O_2 to generate ROS in the presence of calf thymus DNA. The sulfur-based antioxidants are GSH and dimethyl sulfoxide (DMSO) were added to the reaction mixtures in varying orders. By altering the order in which the reagents were allowed to interact with the model system, an interrogation

into the mechanism by with the very prevalent biological antioxidant GSH was explored. It is possible that GSH does not actually protect the cells by ROS scavenging but instead by coordinating to metal ions before they have the opportunity to generate the damaging radical species. Therefore, with this framework, this study set out to better characterize the antioxidant mechanisms of GSH via a comparative study with the known ROS scavenger of DMSO.

3. DESCRIPTION OF THE MODEL

The biological model system used in this study was calf thymus DNA. This DNA was purchased from Sigma-Aldrich and was used without any further purification. The in-vitro experiments performed in these studies also used sulfur based antioxidants that would be typically be found in biological systems (i.e. the reduced form of glutathione, GSH) or behave similarly to biologically relevant antioxidants (DMSO) [7].

Reduced glutathione (γ-L-Glutamyl-L-cysteinylglycine or GSH) is a cysteine-containing tripeptide. GSH is one of the most ubiquitous non-protein bound thiol-containing peptides found in eukaryotic cells [56], usually found in the concentration range of 1–15 mM in the nuclei and 5–11 mM in the mitochondria [3, 9, 57]. Glutathione functions as a major antioxidant, detoxifying many of the endogenous metal-initiated radical species and as essential cofactor for GPx [3]. The ratio of the reduced form to the oxidized form of glutathione, or GSH/GSSG, is a well-accepted indicator of the oxidative stress levels occurring in the cellular environment [56]. In addition to the vast cellular protective functions, Lin et al. showed that glutathione is quite resilient and has been shown to remain viable in *in vitro* studies for extensive time periods, as long as it is stored at near or below freezing temperatures (down to -80°C) [56].

Dimethyl sulfoxide (DMSO), or $(CH_3)_2SO$ [58], was the other organosulfur compound that was used in the present study. The amphiphilic nature of DMSO coupled with the compound's wide range of miscibility in organic solvents, including water, makes it a very versatile solvent in biomedical and chemical research [59]. Yet, reports have also shown DMSO to possess neuroprotective properties in rat brains [59] and to be an effective free radical scavenger [60]. Sanmartín-Suárez et al. showed that DMSO is able to effectively reduce both lipid peroxidation and protein carbonyl formation induced by ferrous chloride/hydrogen peroxide in rat brain

homogenates [59]. The group also showed that DMSO reduced the production of hydroxyl radicals (·OH) during 6-hydroxydopamine autoxidation [59]. While DMSO is indeed a powerful organic solvent, when used at a sufficiently low concentration, between 180–280 mM [59, 61–63], it can successfully be used as an antioxidant on its own or in conjunction with other antioxidants to develop more effective protective therapeutic agents [59].

4. EXPERIMENTAL METHODS

4.1 Overview

A variety analytical methods, including high-pressure liquid chromatography (HPLC) and fluorescence spectroscopy, were used to monitor the degree of oxidative DNA damage and ROS production in the presence and absence of binding interactions between the metals, antioxidant and DNA. The specific antioxidant used in this study was the reduced form of glutathione (98% purity) obtained from Acros Organics and was used without further purification. Calf thymus DNA (sodium salt, type I, highly polymerized), the representative biological DNA model, was also purchased from Sigma-Aldrich® and used without any further purification. The enzymes P_1 nuclease (*Penicillium citrinum*), alkaline phosphatase (bovine, 500 DEA units/mg protein), and catalase (bovine, crystalline suspension in H_2O/0.1% thymol, 21600 units/mg protein) were purchased from Sigma® Life Science.

In addition to the aforementioned analytical techniques, isothermal titration calorimetry (ITC) was also chosen as a means of probing metal ion interactions with the antioxidant. ITC allows for the direct measurement of thermodynamic interaction parameters via the measurement of the heat generated or absorbed when metal ions were allowed to interact with the antioxidant of interest in this study or GSH. The measurements taken from these experiments allows for the measurement of various independent parameters including the binding affinity constant (K_a), the binding enthalpy (ΔH_o), and the binding stoichiometry (n) [64] of the interactions of interest. These parameters can then be seen as the first steps necessary for providing evidence in support of or against whether the sulfur-based antioxidant GSH is capable of ameliorating the damaging effects of ROS

in oxidative DNA damage via metal binding. These parameters can also be used in Equations 1a and 1b to calculate the dependent variables representing Gibbs free energy (ΔG) and the binding entropy (ΔS_o).

$$\Delta G = -RT \ln K_a \qquad \textbf{(1a)}$$

$$\Delta G = \Delta H_o - T\Delta S_o \qquad \textbf{(1b)}$$

The binding enthalpy shows whether the binding reactions are endothermic (positive value) or exothermic (negative value). The magnitude of the binding affinity constant indicates how strongly the titrant and titrand are interacting or simply put how strongly the metal ion of interest interacts with the GSH. The binding stoichiometry value is the ratio of the moles of the metal ion being bound to each mole of GSH. Finally, the binding entropy provides insight into the disorder of the system. For example, an increase in entropy or disorder ($\Delta S_o > 0$) does not provide evidence of metal binding occurring while a decrease in the entropy or disorder ($\Delta S_o < 0$) potentially points to some sort of coordination event occurring since the reaction system is becoming more ordered as the metal binds to the antioxidant. The Gibbs free energy can be calculated to provide a measure of the available energy that can be used to do useful work or how effective the binding processes are for this system.

4.2 Description of GSH and DMSO Concentration Studies

After consulting the literature on the experimental concentrations used in previous studies utilizing GSH and the oxidized form of glutathione (GSSG) [9], as well as typical intracellular concentrations of this naturally occurring biological antioxidant [3], a concentration study was performed. This study serve as a sensitivity analysis for the optimal concentration of GSH that could be used in this study that would allow for quantifiable data to be garnished concerning the reductive effects that GSH had against ROS.

Using a gradually increasing concentration scheme, GSH concentrations ranging from 1.0 μM to 1.0 mM were explored. Each reaction mixture was a total of 500 μL in volume and contained Millipore-grade ultrapure water (resistivity of 18.2 MΩ·cm at 25°C). Each reaction mixture contained 250 μL of 1.0 mg/mL of calf thymus DNA in 240 mM NaCl and 40 mM Tris (pH = 7.0). The metal ions of interest (Cu(I), Cu(II), and Fe(II) in this study) were added at a concentration of 25 μM and the reaction mixtures were allowed to incubate at 37°C for 30 minutes. In the case of the production of the Cu(I) metal ion, sodium ascorbate (NaAsc) and Cu(II) were combined at a 1.25:1 molar ratio. After the incubation step, the corresponding GSH concentrations were added to the reaction mixtures. The last step was the addition of H_2O_2 followed by another incubation period of 1 hour at 37°C.

Catalase (1.0 μL) was added to the reaction mixtures to decompose the H_2O_2 to water and oxygen and quench the reaction. Then 100 μL of a sodium acetate buffer (pH = 5.0) was added to the reaction vessel to prepare the DNA for digestion process for the chromatographic analysis. The DNA was then denatured at 95°C for 5 minutes followed

by rapid cooling on ice. Then 5.0 µL of 1.0 mg/mL P_1 nuclease was added to the reaction mixtures and allowed to incubate overnight at 37°C in order to cleave the phosphodiester bonds in the DNA biopolymer. The reactions were then adjusted to a pH of 8.0 using a Tris buffer and incubated for 8 hours with 1.0 µL of alkaline phosphatase in order to hydrolyze the phosphate groups within each nucleotide.

After analyzing the results of the various concentrations set up for this concentration study, it was determined that the antioxidant concentration that would provide the most biologically relevant results and give a detectable signal would be 0.05 mM of GSH. The DMSO experimental trials also underwent the same type of concentration study. Analysis of the DMSO concentration study showed that the optimal concentration necessary to provide a biologically relevant result was 250 mM of DMSO in each reaction mixture.

4.3 Description of Experimental Procedures for HPLC Studies with GSH

Using the results from the previous concentration study, a set of reactions was run with the optimal GSH concentration. As described in the previous section, each reaction mixture was a total of 500 µL in volume and contained Millipore-grade ultrapure water (resistivity of 18.2 MΩ•cm at 25°C). Each reaction mixture contained 250 µL of 1.0 mg/mL of calf thymus DNA in 240 mM NaCl and 40 mM Tris (pH = 7.0). Under reaction scheme 1 (*Reaction d*), the metal ions of interest were then added to the DNA solution and then the reaction mixtures were allowed to incubate at 37°C for 30 minutes.

Condition 1: $DNA + M^{n+} + preincubation + GSH + H_2O_2 + incubation$ **(d)**

Condition 2: $GSH + M^{n+} + preincubation + DNA + H_2O_2 + incubation$ **(e)**

For the Cu(II) and Fe(II) metal ions, this step was achieved by the addition of 12.5 µL of a 1.0 mM metal solution. In the case of the Cu(I) metal ion, the 12.5 µL of a 1.0 mM Cu(II) and 15.6 µL of a 1.0 mM sodium ascorbate solution had to be combined and allowed to react for five minutes before the addition of the calf thymus DNA. The final concentrations of the metal ions in all the reaction mixtures were 25 µM. The Fe(II) metal solution was freshly made before every experiment using the ferrous iron due to the highly oxidizable nature of the divalent form of iron. After the incubation step, 25 µL of a 1.0 mM GSH solution was added to each reaction vessel, excluding the control reactions, to bring the final concentration of GSH in the reaction mixture to 0.05 mM. Following the addition of GSH, 20 µL of 3% H_2O_2 was added to all the necessary reaction vessels and incubated for

1 hour at 37°C, making the final concentration of hydrogen peroxide in the reaction mixture 35.3 mM.

For reaction scheme 2 (*Reaction e*), the GSH was allowed to interact with the metal ions of interest during the first incubation step before the DNA was added to the reaction containers. The reaction schemes allowed for an examination of the possibility of metal coordination. If metal coordination was occurring in the reactions, then the reactions run using the second set of conditions would yield a statistically significant decrease in the amount of the site-specific damage marker, 8-OH-dG, detected by the HPLC.

The decomposition of the hydrogen peroxide in the reaction mixtures followed the same procedure described in section 4.2. Once the reaction mixtures were ready for chromatographic analysis, 500 µL of each reaction solution was injected into Whatman® Mini-Uniprep™ 0.2-µm syringeless propylene HPLC filter tubes. The use of such a filter ensured that no particulates would clog the HPLC column during the chromatographic separations. All chromatographic separations and analysis for the aforementioned experimental description were performed using a Shimadzu VP Series liquid chromatograph. The setup consisted of a LC-10AT dual pump, a FCV-10AL quaternary low pressure solvent mixer, a SIL-20A HT autosampler, and a SPD-10A dual channel variable wavelength absorption detector (254 nm and 297 nm were the wavelengths of analysis for this study). An ESA Coulochem III ECD at a potential of 280 mV was used to provide on-line electrochemical detection of the 8-OH-dG DNA damage marker. The column used in this study was a Beckman Coulter™ Ultrasphere octadecylsilane (ODS) (45 x 4.6 mm, 5.0 µm particle diameter) with an ODS guard cartridge (4.0 mm x 3.0 mm). The reaction sample injections were 50 µL with a mobile flowrate of 1.0 mL/min and a

24.5-minute sample analysis time. The initial mobile phase composition was 100% water for 30 seconds to focus the sample at the head of the column followed by a linear step gradient to 85 mM ammonium acetate containing 3% acetonitrile. After 7.5 minutes the acetonitrile component was increased to 100% linearly over a 5-minute time period and held at 100% acetonitrile for 4.5 minutes. The mobile phase was then switched back to 100% water for the remaining 7.5 minutes of the sample run in preparation for the next sample injection. The data collected from these experiments was analyzed using the Shimadzu VP Series *EZStart* software version 7.4.

4.4 Description of Experimental Procedures for HPLC Studies with DMSO

Using the results from the results from the previous concentration study, a set of HPLC reactions were run with the optimal DMSO concentration. As described in section 4.3, the same HPLC experimental reaction schemes were used once more with the exception that DMSO was the antioxidant analyzed. To achieve the optimal concentration, each reaction mixture contained a total of 25 μL of a 5.0 M DMSO to a 500 μL total reaction volume. The chromatographic analysis was performed using the same experimental setup and parameters described in section 4.3. The only difference being that the Fe(II)–DMSO experimental trial data was analyzed using an upgraded Shimadzu *LabSolutions* HPLC analysis software package.

4.5 Description of Experimental Procedures for Fluorescence Studies with DMSO

Fluorescence spectroscopy was used to probe the *in vitro* environment to assess how many ROS were being produced when the DMSO was allowed to react with the H_2O_2 in the presence and absence of Cu(II), Fe(II), and Cu(I) using the fluorescent marker 2',7'-dichlorofluorescein (DCF). The fluorescent marker DCF is actually the oxidized form of the native compound dihydrodichlorofluorescein diacetate (DCF-DA), which is a colorless and non-fluorescent molecule [6]. DCF-DA reacts with the ROS in the reaction vessels and is oxidized to form the fluorescent DCF tag. The measure of the fluorescent intensity from these experiments allows for a quantitative measure of the amount of ROS produced when metal ions react with H_2O_2 in the presence and absence of the GSH and DMSO antioxidants.

For the fluorescence studies, each reaction mixture was a total of 1000 µL in volume and contained Millipore-grade ultrapure water (resistivity of 18.2 MΩ•cm at 25°C). Each reaction mixture contained 500 µL of 1.0 mg/mL of calf thymus DNA in 120 mM NaCl and 20 mM Tris (pH = 7.0). A stock solution of the DCF-DA in DMSO (5.0 mg/mL) was diluted by a factor of 2 down to an experimental concentration of 2.5 mg/mL using an equal volume of 0.02 M NaOH. This dilution step allowed the DCF-DA to be properly hydrolyzed by taking off the acetate groups before the fluorescence generating oxidation reactions began. A set of positive control reactions were run first with DNA being combined with the metal ion and incubated at 37°C for 30 minutes before the addition of the DCF-DA hydrogen peroxide. The concentrations of Cu(II), Fe(II), and Cu(I) used were all 25 µM, and the concentration of the H_2O_2 was 0.88 mM. As mentioned in the previous section, Cu(I) was formed by combining 1.0 mM Cu(II) with 1.0 mM sodium ascorbate at a 1.25:1 molar ratio. To prevent photo-oxidation from occurring, all the reactions were run in the absence of direct light.

Under reaction condition 1, the metal ions of interest were added to the DNA solution and the reaction mixtures were allowed to incubate at 37°C for 30 minutes. As previously mentioned, the Fe(II) metal solution was freshly made before every experiment using the ferrous iron due to the highly oxidizable nature of the divalent form of iron. After the incubation step, DMSO was added to each reaction mixture at a concentration of 500 mM followed by the addition of H_2O_2 at a concentration of 0.88 mM. The reaction mixtures were allowed to interact for 1 hour at 37°C. For reaction condition 2, the DMSO was allowed to interact with the metal ions of interest during the first incubation step before the DNA was added to the reaction containers. After the second incubation step, 1.0 µL

catalase was added to the reaction mixtures in order to decompose the H_2O_2 to water and oxygen and quench the reaction.

To carry out fluorescence measurements, each reaction mixture was diluted by a factor of 10. Due to the transient nature of fluorescence, the fluorescence intensity measurements were taken immediately after the catalase was added to the reactions. These measurements were collected using a PerkinElmer LS50B spectrofluorometer. The fluorescence intensity measurements were taken at an excitation wavelength (λ_{ex}) of 503 nm and an emission wavelength (λ_{em}) of 512 nm with a spectral bandwidth of 2.5 nm.

4.6 Description of Experimental Procedures for Fluorescence Studies with GSH

As described in section 4.5, the same fluorescence spectroscopy experimental procedures were used once again with the exception that the antioxidant being used was the GSH. The key difference between the GSH and DMSO fluorescence trials was the GSH concentration which was 50 μM for the GSH case. The fluorescence intensity measurements were performed using the same experimental setup and parameters described in section 4.5.

4.7 Description of Experimental Procedures for ITC Studies with GSH

Isothermal titration calorimetry (ITC) was used to detect the binding interactions of the metals Cu(II), Fe(II), and Cu(I) with the antioxidant GSH. For the ITC measurements both the sample and reference cells contained a total volume of 350 μL and were all run on a TA Instruments Nano ITC Low Volume Isothermal Titration Calorimeter. The ITC instrument was allowed to thermally equilibrate before every experimental run, and each

reaction mixture (reference, sample, and metal titrant) was degassed under vacuum before being placed into the instrument.

After the ITC instrument had been properly cleaned, a volume of 350 μL of Millipore-grade ultrapure water (resistivity of 18.2 MΩ•cm at 25°C) was injected into the reference cell. Then a volume of 300 μL of 0.9 mM GSH in 100 mM Tris (pH = 7.0) was added to the sample cell. The instrument volume injection cap was then placed on the instrument and locked without a titrating syringe in place. The TA Instruments *Launch ITC Run* software package was loaded and automatically recalibrated the zero of the instrument to prevent all of the titrant volume from being injected at once when the experimental trials began. The volume injection cap was fitted with a titrating syringe filled with 50 μL the metal titrant of interest and locked back into place on the instrument. This metal titrant consisted of a 3.2 mM metal solution in 100 mM Tris (pH = 7.0). In the case of the Cu(I) experimental trials, the metal solution consisted of 3.2 mM Cu(II), 4.0 mM sodium ascorbate (NaAsc) in 100 mM Tris (pH = 7.0) in order to keep the aforementioned 1.25:1 molar ratio. The sample cell also contained 0.3 mM GSH and 4.0 mM NaAsc in 100 mM Tris (pH = 7.0) under the Cu(I) trials. The use of the same concentration of NaAsc in the titrant and the titrand allowed for a minimization of unaccounted sources that could contribute to the thermodynamic parameters being measured.

ITC experimental parameters were all specified on the TA Instruments *ITCRun* software package. The experimental setup was run in Incremental Titration mode. This mode had a total of 20 titrant injections separated by a 300 second time interval with each increment consisting of a 2.49 μL injection volume. The stirring rate was 250 rpm with a temperature set-point of 20°C. The program ran auto-equilibrating mode before starting

the experimental trial. This auto-equilibrating mode was used to optimize the slope and standard deviation of the titration isotherm curve to an acceptable limit (m = 0.10 μW/h and st.dev = 0.01 μW). The analysis of the generated isotherms was run using the TA Instruments *NanoAnalyze* software package.

Hydrolyzed and digested DNA samples were analyzed by HPLC. This HPLC-based method measured the radical damage marker, 8-OH-dG, with an electrochemical detector (ECD) and total 2'-deoxyguanosine (dG) with a UV detector (254 nm). Chromatographic analysis was also used to measure the non-radical damage marker, dA *N*-1 oxide, and total 2'-deoxythymidine (dT) via the UV detector (254 nm) as well. The peak area ratio of the 8-OH-dG to dG provides a quantitative and normalized fashion of measuring radical-induced DNA damage, with the larger value indicating a larger amount of that type of damage. Whereas the peak area ratio of the dA *N*-1 oxide to dT can be used to quantify the amount of non-radical induced damage as well as act as a probe for the amount of unreacted H_2O_2 in the reaction vessel. The larger this ratio value, the more non-radical damage accumulated in the system. This type of damage may be accompanied with a large amount or smaller amount of radical-induced damage, depending on the metal ion and reaction condition being used.

Fluorescence spectroscopy experiments were used to probe the *in vitro* environment to assess how much ·OH (a ubiquitous member of the free radical oxygen species group) was being produced when Cu(II), Fe(II), and Cu(I) were allowed to react with the H_2O_2 in the presence and absence of the GSH and DMSO using the fluorescent marker 2',7'-dichlorofluorescein (DCF). Lastly, isothermal titration calorimetry (ITC) was

used to detect the binding interactions of the metals Cu(II), Fe(II), and Cu(I) with the antioxidant GSH.

Each of the experimental trials involving HPLC were run in sets of five while the fluorescence and ITC experiments were run in triplicate. Each experiment set had standard deviations calculated as well as a two sample two-tailed *t*-test at a 95% confidence interval (assuming equal variances) to determine if sample mean differences were statistically significant.

5. RESULTS

5.1 Results of HPLC Studies with GSH

In Figure 3, the peak area ratio for the GSH under experimental conditions 1 and 2 with Cu(II), Fe(II), and Cu(I) are compared to the untreated DNA control conditions with H_2O_2. The peak area ratio is defined as the ratio of the peak area of the radical-induced oxidative DNA damage marker 8-OH-dG to that of the undamaged dG. The area of the peak is proportional to the number of molecules generating the signal. The same definition is applied to the non-radical induced damage peak ratio, wherein the ratio measures DNA damage marker dA *N*-1 oxide to the undamaged dT.

As can be seen in Panel A of Figure 3, both conditions 1 and 2 yield a drastic reduction in the amount of radical-induced oxidative DNA damage when compared to the control not containing any antioxidant. Though all the metal ions tended to yield comparable decreases in the damage marker under both experimental conditions, the Fe(II) experiments tended to form the smallest amount of the 8-OH-dG damage marker even under the untreated experimental conditions.

Panel B of Figure 3 illustrates the amount of non-radical damage (and therefore a probe for the amount of unreacted H_2O_2) that occurs both in the presence and absence of GSH under experimental conditions 1 and 2 for the Cu(II), Fe(II), and Cu(I) metal ions. While both conditions 1 and 2 tended to increase the amounts of non-radical damage for all the metal systems when compared to the control, the Fe(II) system yielded the least pronounced increase but largest overall amount of the non-radical damage marker dA *N*-1 oxide.

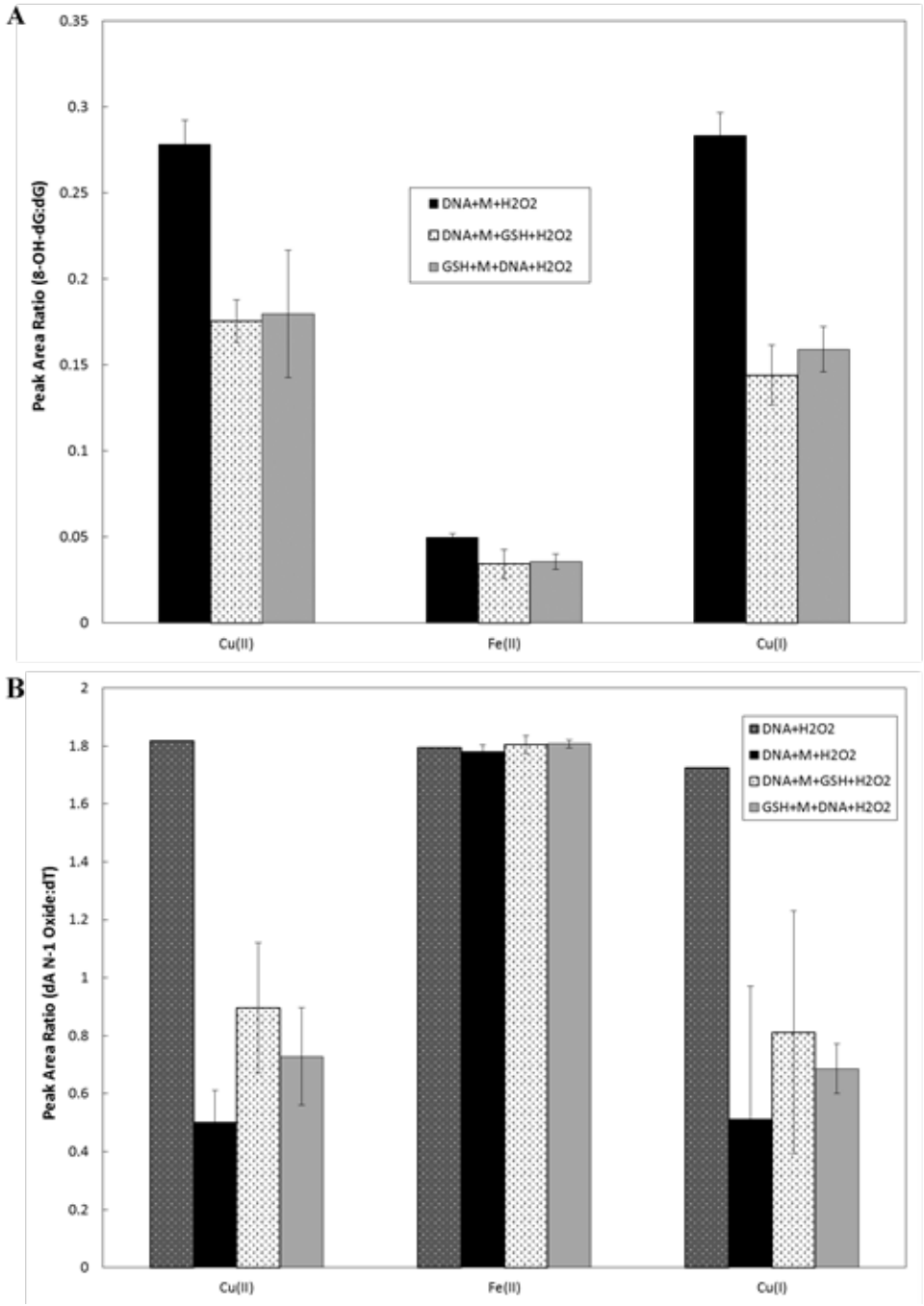

Figure 3. Peak area ratios calculated from HPLC chromatograms show relative molar amounts of 8-OH-dG/dG (panel A) and dA N-1 oxide/dT (panel B) remaining in the reaction vessels after the reactions were allowed to run their course under both experimental conditions. The amounts of the 8-OH-dG/dG decrease for all metals when the antioxidant GSH is used for both experimental conditions 1 and 2. Under Condition 1 the DNA and metal ion of interest were allowed to interact before the addition of the GSH and H_2O_2. Under Condition 2 the GSH and metal ion of interest were allowed to interact before the addition of the DNA and H_2O_2. For the 8-OH-dG/dG measurements, conditions 1 and 2 did not lead to a statistically significant difference in the amount of DNA damage amelioration. Panel B illustrates the degree to which the GSH/Fe(II) system tended to generate the most non-radical damage when compared against the Cu(II) and Cu(I) metal ions using the dA N-1 oxide/dT ratio as a probe of the remaining H_2O_2 in the reactions. The first bar under each metal was included as a negative control for comparative purposes illustrating the amount of H_2O_2 in the reactions before the addition of metal ion. This result is the exact opposite of what can be seen in Panel A when comparing the radical induced damage amongst all the metal ions. The uncertainty bars represent the standard deviation of the average peak area ratio obtained from five trials for each metal ion system.

5.2 Results of HPLC Studies with DMSO

In Figure 4, the peak area ratio for the DMSO under experimental conditions 1 and 2 with Cu(II), Fe(II), and Cu(I) are compared to the untreated DNA control conditions with H_2O_2. The peak area ratio is defined as previously stated in section 5.1. As can be seen in Panel A of the figure, both conditions 1 and 2 yield a marked reduction in the amount of radical-induced oxidative DNA damage when compared to the control, yet not as dramatic of a decrease as was seen in the GSH trials. Panel B of Figure 4 gave a quantitative measurement of the non-radical DNA damage and thus the amount of unreacted H_2O_2 via the dA *N*-1 oxide damage marker. It can be seen that in a similar fashion as the GSH experiments, the DMSO tended to form a larger amount of the dA *N*-1 oxide marker with the Fe(II) metal ion, though not to as drastic a degree as can be seen in Figure 3.

Though all the metal ions tended to yield comparable decreases in the 8-OH-dG damage marker under both experimental conditions, the Fe(II) experiments did tend to form the smallest amount of the damage marker even under the untreated experimental conditions. This result was reflected in the non-radical damage experiments that are summarized in Panel B. By comparing the both the DMSO and GSH trials, it can be seen that the DMSO was not as effective at decreasing the radical-induced DNA damage as GSH when Fe(II) was the metal ion of interest.

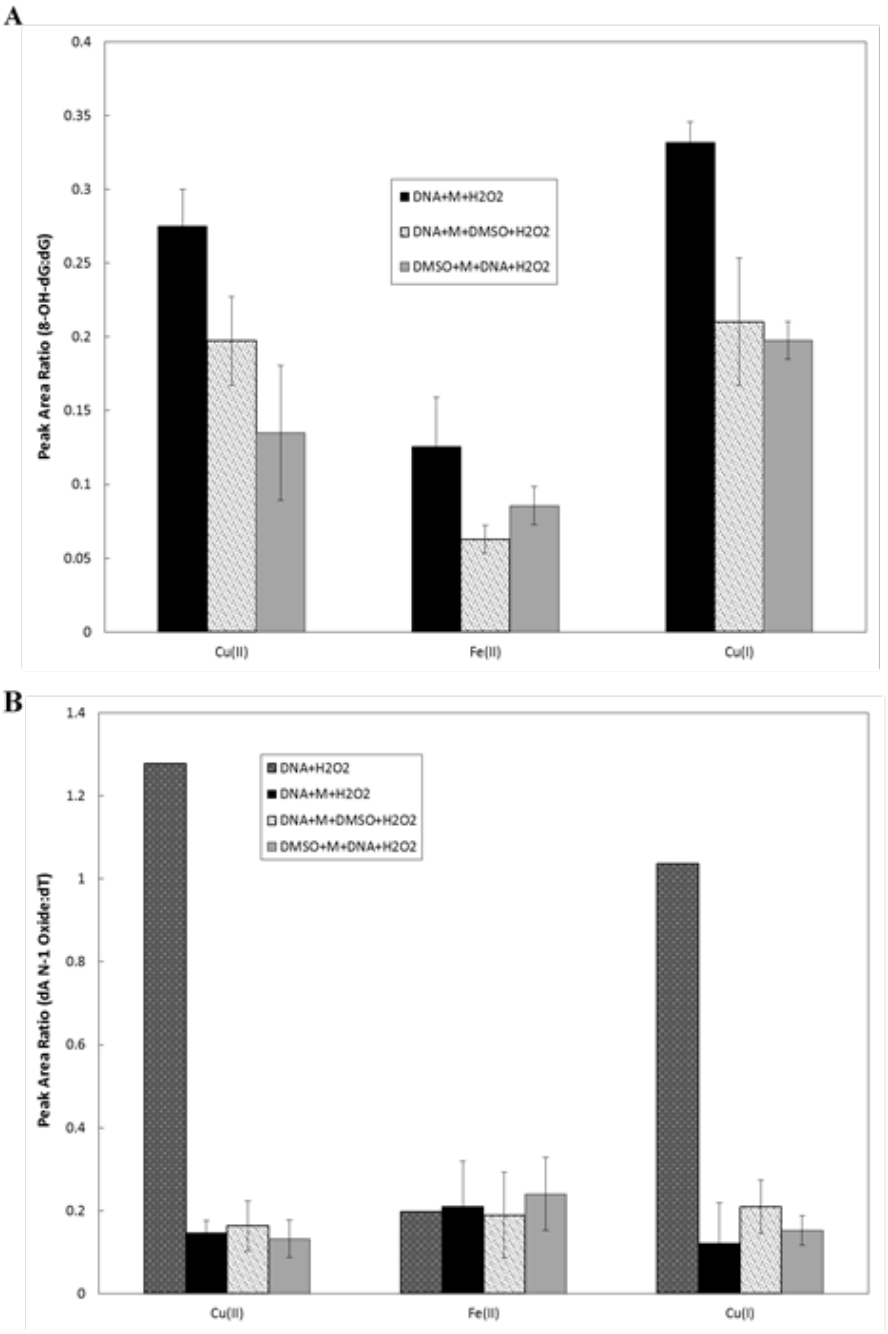

Figure 4. Peak area ratios calculated from HPLC chromatograms show relative molar amounts of 8-OH-dG/dG (panel A) and dA N-1 oxide/dT (panel B) remaining in the reaction vessels after the reactions were allowed to run their course under both experimental conditions. The amounts of the 8-OH-dG/dG decrease for all metals when the antioxidant DMSO is used for both experimental conditions 1 and 2. Under Condition 1 the DNA and metal ion of interest were allowed to interact before the addition of the DMSO and H_2O_2. Under Condition 2 the DMSO and metal ion of interest were allowed to interact before the addition of the DNA and H_2O_2. For the 8-OH-dG/dG measurements, conditions 1 and 2 did yield a statistically significant difference in the amount of DNA damage amelioration for the Cu(II) and Fe(II) metal ions but not for the Cu(I) metal ion. Panel B shows the level to which the metal-DMSO systems tended to generate non-radical DNA damage using the dA N-1 oxide/dT ratio as a probe of the remaining H_2O_2 in the reactions. The first bar under each metal was included as a negative control for comparative purposes illustrating the amount of H_2O_2 in the reactions before the addition of metal ion. These results tended to reciprocate the results from Panel A – i.e. a smaller amount radical-induced damage correlated with a larger amount of non-radical damage. The uncertainty bars represent the standard deviation of the average peak area ratio obtained from five trials for each metal ion system.

The results from all the HPLC radical-induced damage measurements (for both GSH and DMSO) are summarized in Table 1 shown below. Under conditions 1 and 2, the GSH performed very comparably in terms of 8-OH-dG reduction. However, the DMSO performed better under condition 2 than condition 1 for the Cu(II) metal ion experiments to a statistically significant level (51 ± 25% versus 28 ± 13% respectively). While the opposite occurred for the Fe(II) metal ion experiments, where DMSO performed to a statistically significant level under experimental condition 1 than condition 2 (50 ± 13% versus 32 ± 13% respectively). The peak area ratios reported in the table are multiplied by a factor of a 1000 for scaling purposes.

Table 2 below summarizes the results from all the HPLC non-radical induced damage measurements for both GSH and DMSO. Under conditions 1 and 2, the DMSO performed very comparably in terms of the dA *N*-1 oxide generation for the Cu(II) and Fe(II) metal systems. However, the DMSO did not generate a statistically significant amount of the dA *N*-1 marker under condition 1 than condition 2 for any of the metal ion experiments (-75 ± 22% versus -25 ± 21% respectively). The GSH tended to generate comparable amounts of the dA *N*-1 oxide marker for all the metal systems and yielded no statistically significant differences in the non-radical damage marker under each reaction scheme for all metal ion systems.

Table 1.
Effects of GSH and DMSO on radical-induced oxidative DNA damage for the reactions using Cu(II), Fe(II), and Cu(I) with H_2O_2. The peak area ratios of the 8-OH-dG/dG x 1000 are reported. Values in parentheses indicate the percentage decrease of the peak area ratio using GSH or DMSO relative to the untreated ($M^{n+} + H_2O_2$) control reaction condition.

	Controls		Condition 1[a]		Condition 2[b]	
	$M^{n+} + H_2O_2$[y]	$M^{n+} + H_2O_2$[z]	GSH	DMSO	GSH	DMSO
Cu(II)	278 ± 14	275 ± 25	175 ± 13 (37 ± 7%)	197 ± 30[c] (28 ± 13%)	180 ± 37 (35 ± 17%)	135 ± 46[c] (51 ± 25%)
Fe(II)	50 ± 2	126 ± 34	34 ± 8 (32 ± 19%)	63 ± 9[c] (50 ± 13%)	36 ± 4 (28 ± 10%)	86 ± 13[c] (32 ± 13%)
Cu(I)	283 ± 13	332 ± 14	144 ± 17 (49 ± 11%)	210 ± 43 (37 ± 17%)	159 ± 13 (44 ± 8%)	198 ± 13 (41 ± 6%)

[a] Experimental Condition 1: DNA + M^{n+} + GSH or DMSO + H_2O_2
[b] Experimental Condition 2: GSH or DMSO + M^{n+} + DNA + H_2O_2
[c] Indicates that there was a statistically significant difference between experimental conditions 1 and 2 using DMSO
[y] Control values from GSH experiments
[z] Control values from DMSO experiments

Table 2.
Effects of GSH and DMSO on non-radical induced oxidative DNA damage for the reactions using Cu(II), Fe(II), and Cu(I) with H_2O_2. The peak area ratios of the dA *N*-1 oxide/dT are reported. Values in parentheses indicate the percentage decrease of the peak area ratio using GSH or DMSO relative to the untreated ($M^{n+} + H_2O_2$) control reaction condition.

	Controls		Condition 1[a]		Condition 2[b]	
	$M^{n+} + H_2O_2$[y]	$M^{n+} + H_2O_2$[z]	GSH	DMSO	GSH	DMSO
Cu(II)	0.50 ± 0.11	0.15 ± 0.03	0.90 ± 0.23 (-80 ± 20%)	0.16 ± 0.06 (-7 ± 27%)	0.73 ± 0.17 (-46 ± 19%)	0.13 ± 0.05 (13 ± 28%)
Fe(II)	1.78 ± 0.02	0.21 ± 0.11	1.81 ± 0.03 (-2 ± 2%)	0.19 ± 0.10 (10 ± 34%)	1.81 ± 0.01 (-2 ± 1%)	0.24 ± 0.09 (-14 ± 27%)
Cu(I)	0.51 ± 0.46	0.12 ± 0.10	0.81 ± 0.42 (-59 ± 34%)	0.21 ± 0.06 (-75 ± 22%)	0.69 ± 0.09 (-35 ± 12%)	0.15 ± 0.04 (-25 ± 21%)

[a] Experimental Condition 1: DNA + M^{n+} + GSH or DMSO + H_2O_2
[b] Experimental Condition 2: GSH or DMSO + M^{n+} + DNA + H_2O_2
[y] Control values from GSH experiments
[z] Control values from DMSO experiments

5.3 Results of Fluorescence Studies with GSH

Figure 5 illustrates the relative fluorescence of the fluorescent probe DCF in reactions involving DNA and the metal ions Cu(II), Fe(II), or Cu(I) in the presence and absence of GSH and activated with H_2O_2. The goal of the experiment was to probe the reaction environment and observe the relative amounts of ROS production and correlate them with the HPLC studies. In these sets of studies, the larger relative fluorescence intensity values were indicative of more ROS being generated under the experimental condition being examined. As can be seen in the figure, both conditions 1 and 2 yield a pronounced reduction in the amount of ROS produced when compared to the control for the Cu(II) and Cu(I) metal ions. The copper metal systems tended to form the largest amounts of oxidative DNA damage which was consistent with the results from the HPLC trials.

Although the Fe(II) experiments did tend to form the smallest amount of the damage marker even under the untreated experimental conditions, the trials did seem to exhibit a strange phenomenon wherein the relative DCF fluorescence intensity actually increased when treated with GSH as compared to the control. Overall, experimental conditions 1 and 2 did yield a statistically significant difference for this phenomenon as well as the other metal ions when treated with GSH.

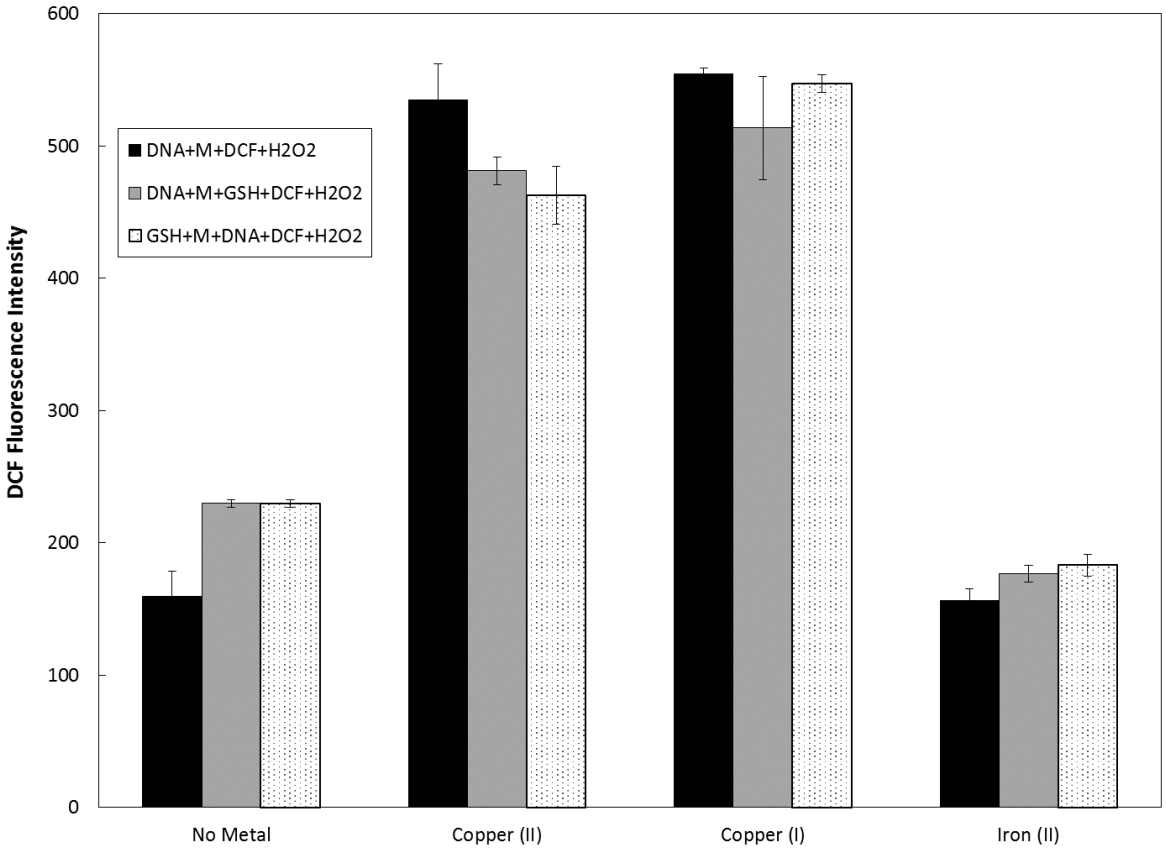

Figure 5. DCF fluorescence intensities show relative amounts of ROS in the reaction vessels after the reactions were allowed to run their course under both experimental conditions. The 'no metal' reaction conditions were negative controls used to give a measure of drastic the effects of metal-mediated oxidative damage were on ROS production. As can be seen, the amounts of the ROS generated decreased when GSH was added to the Cu(II) and Cu(I), but actually increased when the metal of interest was Fe(II) for both experimental conditions 1 and 2. Under Condition 1 the DNA and metal ion of interest were allowed to interact before the addition of the GSH, DCF and H_2O_2. Under Condition 2 the GSH and metal ion of interest were allowed to interact before the addition of the DNA, DCF and H_2O_2. For the GSH fluorescence experiments conditions 1 and 2 did yield a statistically significant difference in the amount of DNA damage amelioration for the Cu(II), Fe(II), and the Cu(I) metal ions. For comparison purposes, the GSH experimental results were performed by another individual in the lab. The uncertainty bars represent the standard deviation of the average DCF fluorescence obtained from five trials for each metal ion system.

5.4 Results of Fluorescence Studies with DMSO

Figure 6 illustrates the relative fluorescence of the fluorescent probe DCF in reactions involving DNA and the metal ions Cu(II), Fe(II), and Cu(I) in the presence and absence of DMSO and activated with H_2O_2. As can be seen in the figure, both conditions 1 and 2 yield a pronounced reduction in the amount of radical-induced oxidative DNA damage when compared to the control for the Cu(II) and Cu(I) metal ions and an even more drastic reduction in the Fe(II) metal system. The copper metal systems tended to form the largest amounts of oxidative DNA damage which was consistent with the results from the HPLC trials.

However, comparing the both the DMSO and GSH trials, it can be seen that the DMSO was actually more effective at decreasing the radical-induced DNA damage than the GSH which is in stark contrast to the results obtained from the HPLC experiments. For both oxidation states of the copper metal, a statistically significant difference could be seen in the reduction of the ROS generation under Condition 2 compared to Condition 1 (52 ± 11% versus 13 ± 3% for Cu(II) and 13 ± 4% versus 11 ± 1% for Cu(I) respectively).

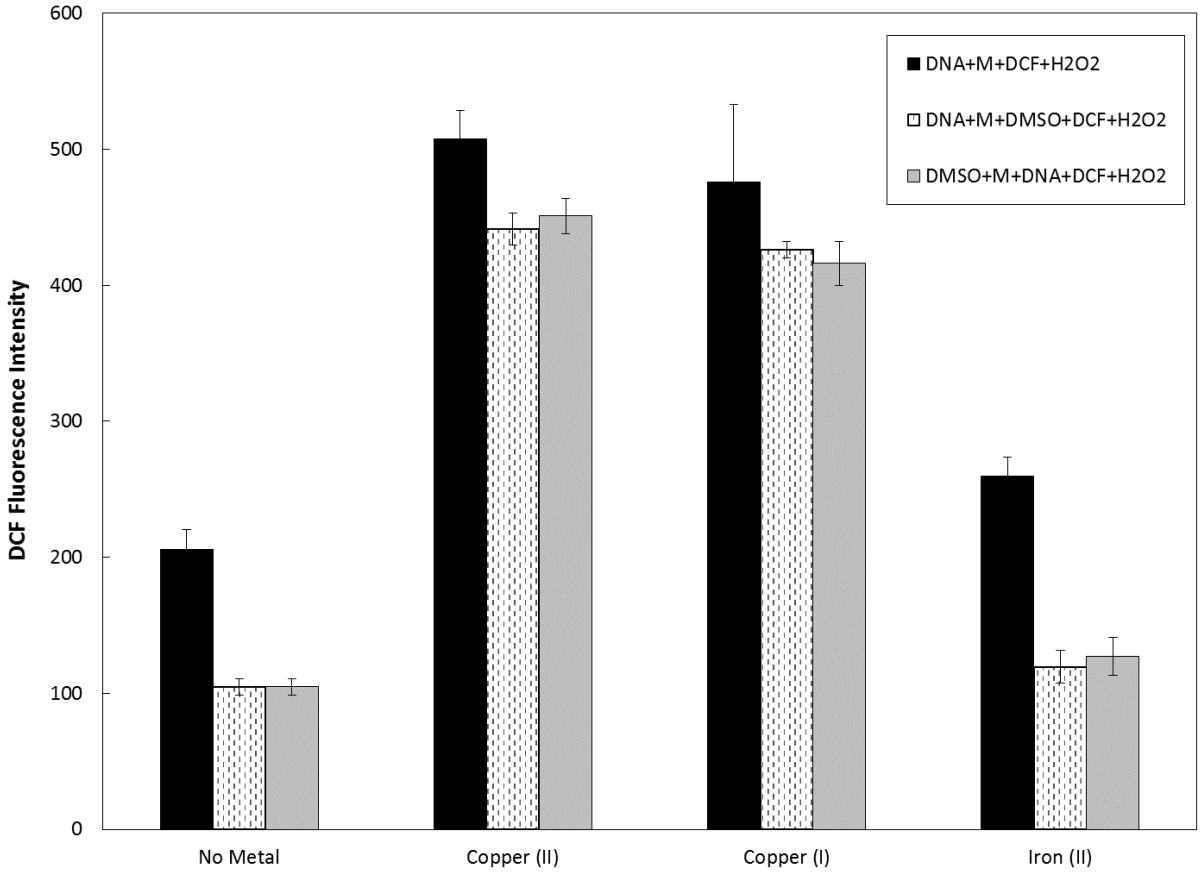

Figure 6. DCF fluorescence intensities show relative amounts of ROS in the reaction vessels after the reactions were allowed to run their course under both experimental conditions. The 'no metal' reaction conditions were negative controls used to give a measure of drastic the effects of metal-mediated oxidative damage were on ROS production. As can be seen, the amounts of the ROS generated decreased when GSH was added to the Cu(II) and Cu(I), and significantly decreased when the metal of interest was Fe(II) for both experimental conditions 1 and 2. Under Condition 1 the DNA and metal ion of interest were allowed to interact before the addition of the GSH, DCF and H_2O_2. Under Condition 2 the DMSO and metal ion of interest were allowed to interact before the addition of the DNA, DCF and H_2O_2. For the DMSO fluorescence experiments conditions 1 and 2 did yield a statistically significant difference in the amount of DNA damage amelioration for the Cu(II) and Cu(I) metal ions but not for the Fe(II) metal ion. The uncertainty bars represent the standard deviation of the average DCF fluorescence obtained from five trials for each metal ion system.

The results from all the fluorescence trials (for both GSH and DMSO) are summarized in Table 3 shown below. Under conditions 1 and 2, the GSH performed comparably in terms of ROS reduction for all metals except the Cu(I) metal ion. While the GSH did have a statistically significant difference under conditions 1 and 2 for all metal ions, it had a marked difference for the Cu(I) ion (7 ± 7% versus 1 ± 1% respectively). Only when the metal ion being used was the Fe(II) did the GSH actually seem to actually raise ROS levels relative to the control for both experimental conditions. However, the DMSO performed slightly better under condition 1 than condition 2 for the Fe(II) metal ion experiments (79 ± 9% versus 51 ± 10% respectively). While the opposite occurred for the Cu(II) metal ion experiments, where DMSO performed significantly more favorably under experimental condition 2 than condition 1 (52 ± 11% versus 13 ± 3% respectively). The ROS levels are reported as relative levels of DCF fluorescence intensity for all experimental conditions for both the GSH and DMSO antioxidants.

Table 3.
Effects of GSH and DMSO on DCF fluorescence intensities for the reactions using Cu(II), Fe(II), and Cu(I) with H_2O_2. The DCF fluorescence intensities reported represent the relative ROS levels left in the reaction after the experiment. Values in parentheses indicate the percentage decrease or increase in the ROS levels using GSH or DMSO relative to the untreated (M^{n+} + DCF + H_2O_2) control reaction condition.

	Controls		Condition 1[a]		Condition 2[b]	
	M^{n+} + DCF + H_2O_2[y]	M^{n+} + DCF + H_2O_2[z]	GSH	DMSO	GSH	DMSO
Cu(II)	535 ± 27	508 ± 21	481 ± 10[c] (10 ± 2%)	442 ± 12[d] (13 ± 3%)	462 ± 22[c] (14 ± 5%)	450 ± 13[d] (52 ± 11%)
Fe(II)	156 ± 9	260 ± 14	177 ± 6[c] (-13 ± 3%)	119 ± 12 (79 ± 9%)	183 ± 8[c] (-17 ± 4%)	127 ± 14 (51 ± 10%)
Cu(I)	554 ± 5	476 ± 57	514 ± 39[c] (7 ± 7%)	426 ± 6[d] (11 ± 1%)	547 ± 7[c] (1 ± 1%)	416 ± 16[d] (13 ± 4%)

[a] Experimental Condition 1: DNA + M^{n+} + GSH or DMSO+ DCF + H_2O_2
[b] Experimental Condition 2: GSH or DMSO + M^{n+} + DNA + DCF + H_2O_2
[c] Indicates there was a statistically significant difference between experimental conditions 1 and 2 using GSH
[d] Indicates that there was a statistically significant difference between experimental conditions 1 and 2 using DMSO
[y] Control values from GSH experiments
[z] Control values from DMSO experiments

5.5 Results of GSH Metal Binding Studies using ITC

Though the HPLC and fluorescence results were consistent with each other for both the antioxidants of interest in this study, concluding whether GSH behaves as a radical scavenger or uses a metal coordination scheme is difficult to say unequivocally. If metal ion binding is the mechanism of execution, one would expect condition 2 would yield a statistically significant difference in the lowering of radical-induced damage marker over condition 1. This expectation would stem from the fact that the GSH is allowed to interact with the metal ion of interest during the pre-incubation step before the DNA and H_2O_2 are introduced into the system. Such an outcome was not observed from the HPLC experiments suggesting that metal binding may not be the mechanism by which GSH is able to alleviate the damaging effects of radical-induced oxidative DNA damage.

Thus, isothermal titration calorimetry (ITC) experiments were used to interrogate the GSH ameliorating effects against metal-mediated oxidative damage and explore whether the antioxidant had a positive binding interactions with the metal ions of interest. ITC serves as a method of providing a more independent interpretation of whether metal binding is occurring with GSH.

In Figures 7–9 overleaf, ITC binding studies were conducted for the Cu(II), Fe(II), and Cu(I) metal ion systems with the antioxidant GSH. The mole ratios reported are those of the metal ion to antioxidant (i.e. M^{n+}:GSH). Each set of ratios begin at low dilutions and are increased until the solubility limit is reached. Each experiment consisted of consisted of 20 titrant injections of a 3.2 mM metal solution into a 0.9 mM GSH solution, which resulted in the isotherms that can be seen in Panel A in all the following figures. The *NanoAnalyze* software package was then used to fit the data to the *Independent* binding model using a non-linear least squares method. This binding model was then used to generate the best-fit values for the binding stoichiometry (*n*), binding

affinity constant (K_a), enthalpy of binding (ΔH_o), and entropy of binding (ΔS_o) [65–67]. Since all the binding studies were run in triplicate, a representative isotherm and binding model fit are presented for each metal system.

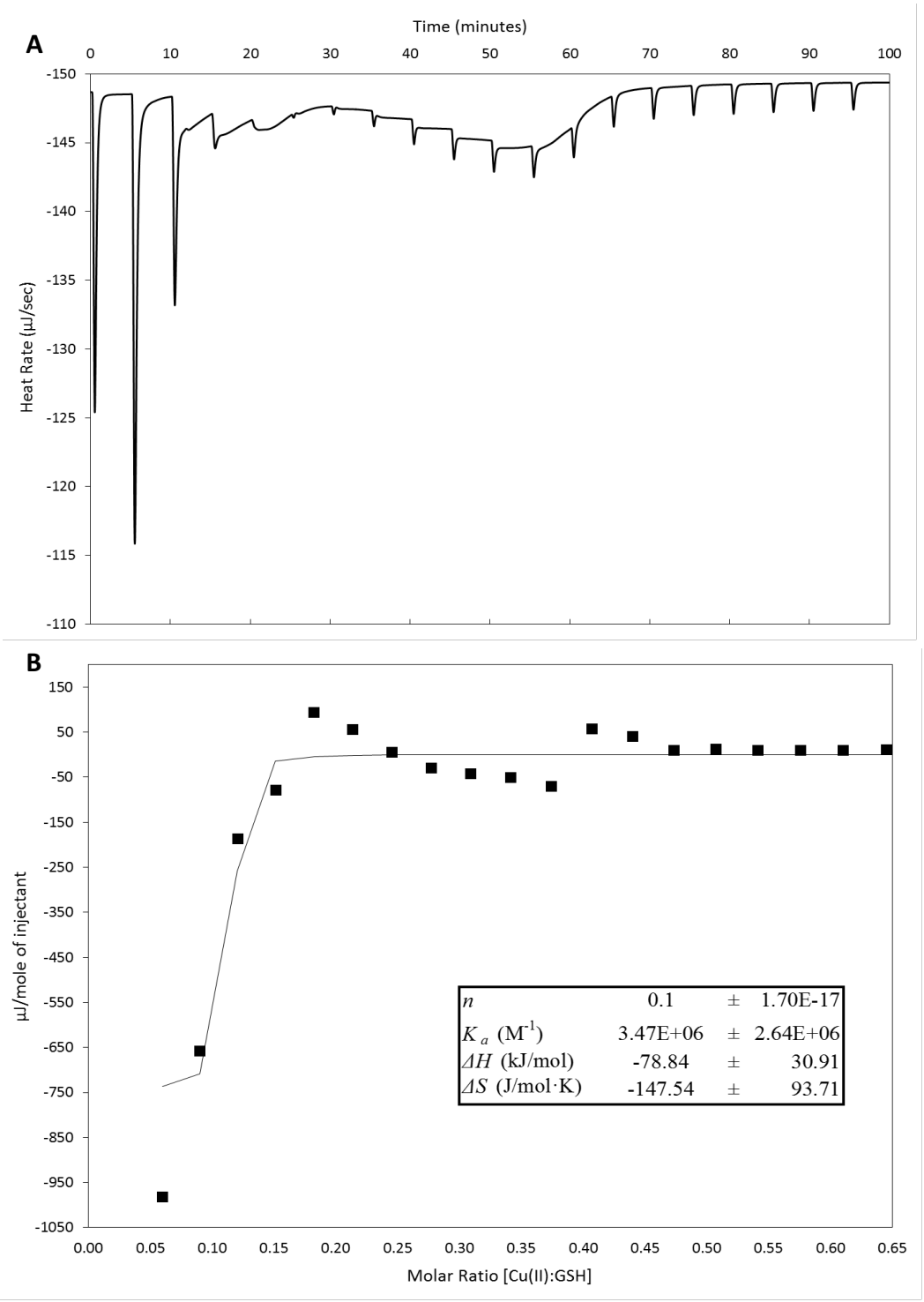

Figure 7. Representative ITC binding curve for the experimental run with 20 equal injections of a 3.2 mM Cu(II) solution being titrated into 0.9 mM GSH titrand solution run at 20°C. Panel A displays the raw ITC isotherm after the buffer heat effects are subtracted from the raw data. Panel B illustrates the non-linear least squares fit of the peak area data from Panel A to the Independent binding model. Panel B also contains the independent thermodynamic parameters, n, K_a, ΔH, and the dependent parameter, ΔS, with their associated standard deviations from the triplicate experimental run.

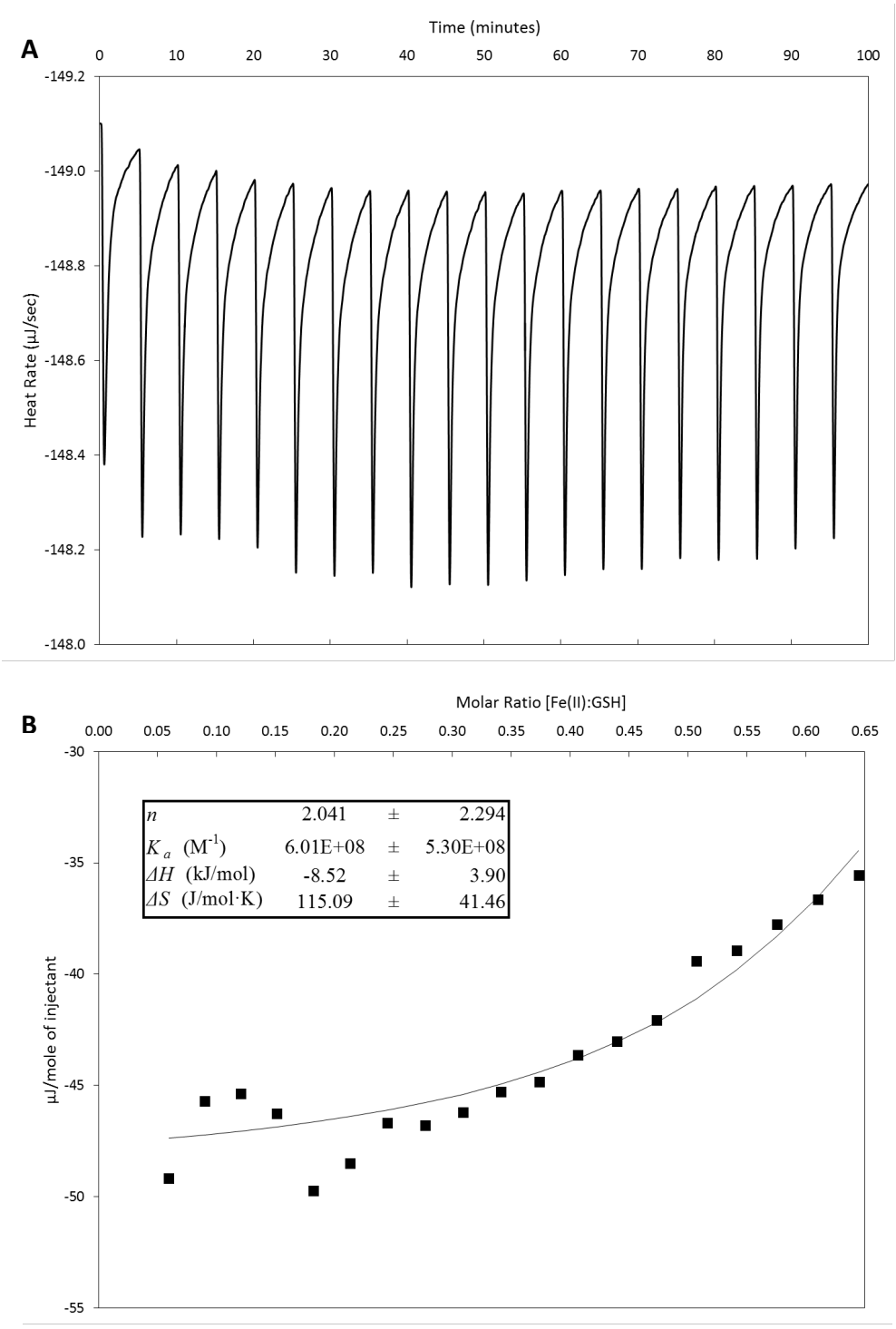

Figure 8. Representative ITC binding curve for the experimental run with 20 equal injections of a 3.2 mM Fe(II) solution being titrated into 0.9 mM GSH titrand solution run at 20°C. Panel A displays the raw ITC isotherm after the buffer heat effects are subtracted from the raw data. Panel B illustrates the non-linear least squares fit of the peak area data from Panel A to the Independent binding model. Panel B also contains the independent thermodynamic parameters, n, K_a, ΔH, and the dependent parameter, ΔS, with their associated standard deviations from the triplicate experimental run.

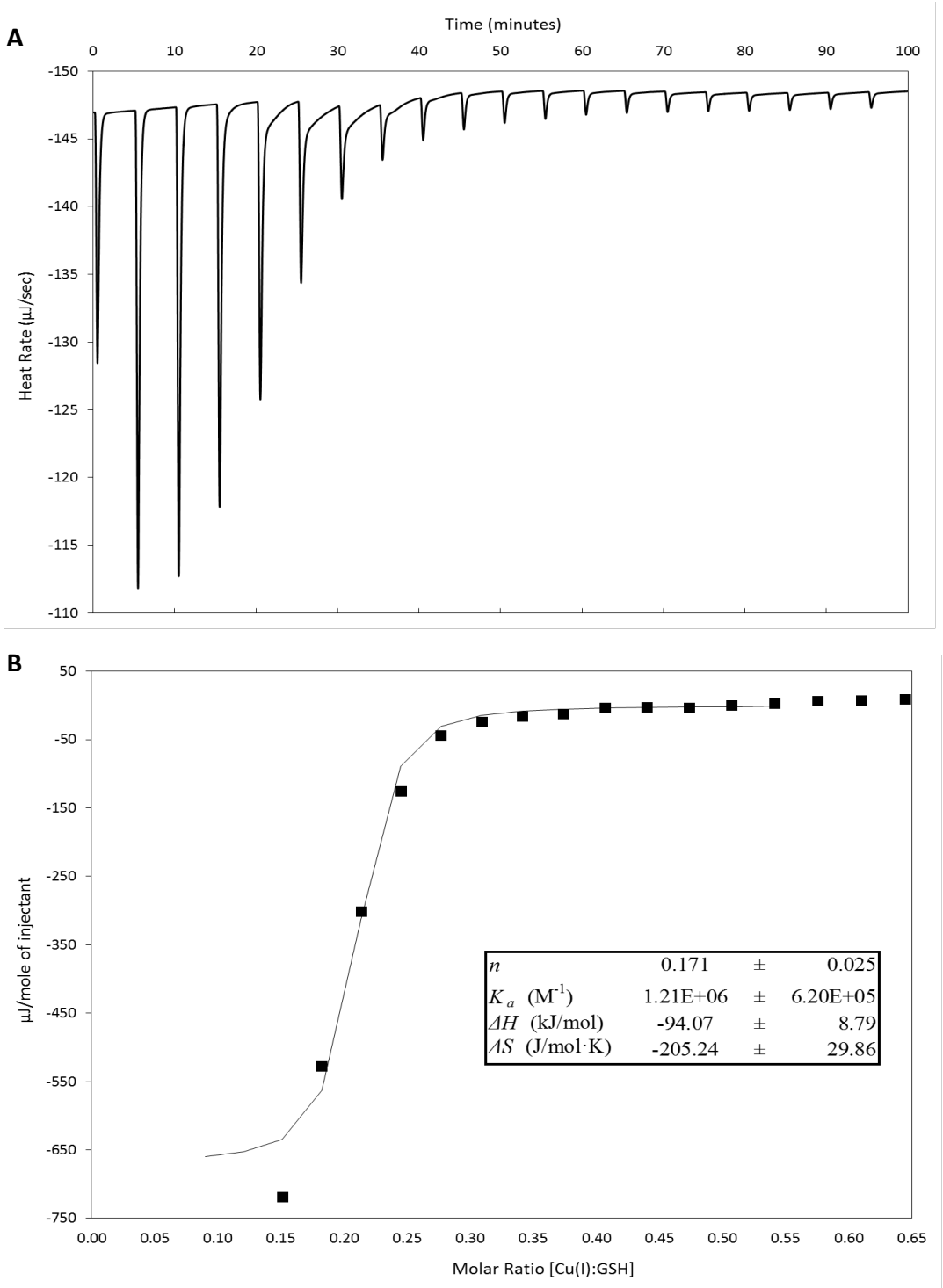

Figure 9. Representative ITC binding curve for the experimental run with 20 equal injections of a 3.2 mM Cu(I) solution being titrated into 0.9 mM GSH titrand solution run at 20°C. Panel A displays the raw ITC isotherm after the buffer heat effects are subtracted from the raw data. Panel B illustrates the non-linear least squares fit of the peak area data from Panel A to the Independent binding model. Panel B also contains the independent thermodynamic parameters, n, K_a, ΔH, and the dependent parameter, ΔS, with their associated standard deviations from the triplicate experimental run.

Table 4 below summarizes all the independent variables (n, K_a, and ΔH_o) calculated from the Independent binding model for the Cu(II), Fe(II), and Cu(II) metal ions with the GSH antioxidant binding studies. The dependent variables for the binding entropy (ΔS_o) and the Gibbs free energy (ΔG) are also reported. The ΔS_o values were calculated using the Independent binding model while the ΔG values were calculated using Equation 1a. Standard deviations for each parameter are also reported.

Table 4.
Binding parameters from the ITC metal coordination studies using the Cu(II), Fe(II), and Cu(I) metal titrant with the GSH titrand are summarized. The binding stoichiometry (n), binding affinity constant (K_a), enthalpy of binding (ΔH_o), entropy of binding (ΔS_o) and Gibbs free energy of binding (ΔG) are reported with their associated errors. All values reported are from experiments run in triplicate at an experimental temperature of 20°C.

	n	**K_a (M^{-1})**	**ΔH_o (kJ/mol)**	**ΔS_o (J/mol·K)**	**ΔG (kJ/mol)**
Cu(II)	0.10 ± 0.00	$3.47 \times 10^6 \pm 1.71 \times 10^6$	-78.84 ± 30.91	-147.54 ± 93.71	-35.59 ± 3.47
Fe(II)	2.04 ± 2.29	$6.01 \times 10^8 \pm 5.30 \times 10^8$	-8.52 ± 3.90	115.09 ± 41.46	-42.26 ± 13.82
Cu(I)	0.17 ± 0.03	$1.21 \times 10^6 \pm 6.20 \times 10^5$	-94.07 ± 8.79	-205.24 ± 29.86	-33.91 ± 1.29

6. DISCUSSION

In order to provide an easier method of evaluating the results from the HPLC and fluorescence studies, Tables 5, 6, and 7 summarize the trends observed in the 8-OH-dG levels and ROS production. To this end, an upwards pointing arrow and a downward pointing arrow are used to represent when the result of the particular experiment lead to a statistically significant (unless otherwise marked) increase or decrease in the parameter being evaluated when compared to the untreated control conditions. Any statistically significant differences between experimental conditions 1 and 2 for the HPLC and fluorescence studies are also reported.

Tables 5–6 provide a qualitative interpretation of the trends that emerged from the radical-induced and non-radical induced oxidative DNA damage trials using chromatographic analysis from the HPLC experiments (i.e. Figures 3–6). Experimental conditions 1 and 2 were interrogated for both the radical-induced (8-OH-dG) and the non-radical induced (dA *N*-1 oxide) damage cases for both the GSH and DMSO. The next table (Table 7) illustrates the trends in overall ROS production based on the fluorescence studies. The arrow directions in the table correspond to the relative fluorescence intensity of the DCF-DA, which is the fluorescent probe that is used to quantify how much ROS are being generated under each experimental condition in the presence and absence of the antioxidant of interest.

Table 5.
Qualitative look at the effects of GSH and DMSO on radical-induced oxidative DNA damage due to metal ion mediation in the presence of H_2O_2. The directions of the arrow indicate whether the antioxidant of interest decreases or increases the amount of the radical damage marker 8-OH-dG.

	GSH		**DMSO**	
	Condition 1[a]	Condition 2[b]	Condition 1[a]	Condition 2[b]
Cu(II)	↓	↓	↓	↓‡
Fe(II)	↓	↓	↓†	↓
Cu(I)	↓	↓	↓	↓

[a] Experimental Condition 1: DNA + M^{n+} + GSH or DMSO + H_2O_2
[b] Experimental Condition 2: GSH or DMSO + M^{n+} + DNA + H_2O_2
† Indicates that condition 1 lowered the amount of 8-OH-dG generation to a statistically significant lower level than condition 2 using DMSO
‡ Indicates that condition 2 lowered the amount of 8-OH-dG generation to a statistically significant lower level than condition 1 using DMSO

Table 6.
Qualitative look at the effects of GSH and DMSO on non-radical induced oxidative DNA damage due to metal ion mediation in the presence of H_2O_2. The directions of the arrow indicate whether the antioxidant of interest decreases or increases the amount of the non-radical damage marker dA *N*-1 oxide.

	GSH		**DMSO**	
	Condition 1[a]	Condition 2[b]	Condition 1[a]	Condition 2[b]
Cu(II)	--	--	--	--
Fe(II)	--	--	--	--
Cu(I)	--	--	--	--

[a] Experimental Condition 1: DNA + M^{n+} + GSH or DMSO + H_2O_2

[b] Experimental Condition 2: GSH or DMSO + M^{n+} + DNA + H_2O_2

[- -] Indicates that the experimental condition did not increase or decrease the dA *N*-1 oxide to a statistically significant level when compared against the untreated DNA control

Table 7.
Qualitative look at the effects of GSH and DMSO on free radical species ·OH via relative fluorescence intensity. The directions of the arrow indicate whether the antioxidant of interest decreases or increases the amount of the relative DCF fluorescence intensity.

	GSH		DMSO	
	Condition 1[a]	Condition 2[b]	Condition 1[a]	Condition 2[b]
Cu(II)	↓	↓†	↓*	↓
Fe(II)	↑	↑†	↓	↓
Cu(I)	↓*	↓	↓	↓†

[a] Experimental Condition 1: DNA + M^{n+} + GSH or DMSO+ DCF + H_2O_2

[b] Experimental Condition 2: GSH or DMSO + M^{n+} + DNA + DCF + H_2O_2

[*] Indicates that condition 1 increased or lowered the amount of DCF fluorescence to a statistically significant lower level than condition 2 using the antioxidant of interest

[†] Indicates that condition 2 lowered the amount of DCF fluorescence to a statistically significant lower level than condition 1 using the antioxidant of interest

The tables from the last few pages serve a few purposes. First, they strive to answer the overarching question of this study concerning the antioxidant mechanism of the reduced form of glutathione: does GSH behave similarly to DMSO (i.e. as a free radical scavenger)? Or is the method of amelioration of the oxidative DNA damage due to metal coordination? Closer examination of the trends that arose from each of the experiments may provide evidence supporting that GSH may behave as a free radical scavenger with some metal systems while using metal coordination with other metal ions. It is also possible that the true mechanism will possibly be a combination of these two methods.

The general trend that one would expect from these experiments would include a reduction in the 8-OH-dG generation, which would correspond to 'down' arrows in Table 5. The 8-OH-dG is a damage marker due to ROS producing oxidative damage at or near the guanine base. Therefore, one would expect that any 'down' arrow from Table 5 would correspond to a 'down' arrow in Table 7 since the fluorescence studies were a way to measure the ROS production in the reaction vessel. Table 6 looks at the non-radical damage trends. Therefore, one would expect that a lower value or a 'down' arrow in Table 5 could possibly correspond to an 'up' arrow in Table 6 if the antioxidant is only able to prevent the metal ion of interest from interacting with the peroxide and generating the harmful ROS but not completely stopping DNA damage from occurring. An 'up' arrow in Table 6 also demonstrates that excess peroxide is available for causing non-radical damage, which should correlate with less radical-induced damage.

Upon examination of Table 5 and 7, it can be seen that when the antioxidant was GSH, condition 2 lowered the DCF fluorescence by a statistically significant level when compared to condition 1 for the Cu(II) metal ion. This is consistent with Cu(II) forming a coordination complex with GSH and behaving as an antioxidant by decreasing metal-mediated ROS production. For the

Cu(I) metal ion system, the opposite trend was observed, with condition 1 yielding the statistically significant difference in the lowering of the ROS production. The Fe(II) metal ion system yielded a different observation with the addition of the GSH actually increasing the ROS production to a statistically significant level for condition 2. This result could be viewed as evidence that at the concentration of GSH being used for the Fe(II) system, GSH actually displays pro-oxidant capabilities. For the DMSO fluorescence experiment, lowered ROS production was observed for all metal systems, with reaction scheme 1 lowering the observed DCF fluorescence to a statistically significant level for Cu(II) while reaction scheme 2 did so for the Cu(I) metal system. The Fe(II) system did not generate a statistically significant lower signal under either reaction condition for any of the metal systems.

The ROS production experiment results are in stark contrast to Table 5, where conditions 1 and 2 did not yield a statistically significant difference in the reduction of the 8-OH-dG damage marker for the GSH, suggesting that metal coordination might not be the main mechanism by which GSH operates. When the antioxidant being used was DMSO, only conditions 2 for Cu(II) and 1 for Fe(II) lead to a statistically significant decrease in the 8-OH-dG marker. Such opposing results raise an interesting point about how metal-dependent the free radical scavenging mechanism is when it comes to ameliorating the damaging effects of radical-induced oxidative DNA damage.

Examination of Table 6 reveals that neither the GSH nor DMSO antioxidants generated a statistically significant increase in the dA *N*-1 oxide non-radical damage marker for either of the two reaction schemes. One would expect that if the antioxidant were preventing the metal ions from being activated by the hydrogen peroxide by coordinating to the metal ion, then the decrease in radical-induced damage would correlate to an increase in the non-radical damage marker

observed since there would be unreacted H_2O_2 left in the system. Since such an event was not observed for either antioxidant, it could not be conclusively stated that the GSH was lowering the radical-induced oxidative DNA damage via a metal coordination mechanism.

Based on the results from the oxidative damage marker studies with GSH and DMSO, there is evidence that metal coordination may not be a method by which GSH ameliorates the damaging effects of free radical production, or at the very least, not the main technique the antioxidant uses. However, DMSO did have a few cases in which there was a statistically significant decrease in the 8-OH-dG levels between conditions 1 and 2 (i.e. Cu(II) and Fe(II)). These differences for DMSO were surprising since DMSO tends to behave as a radical scavenger, yet these results appear to indicate that DMSO may use metal coordination in conjunction with radical scavenging for the Cu(II) metal ion in order to prevent the ROS formation.

The results from the ITC studies sought to provide a more concise and independent evaluation of possible metal coordination interactions with GSH. In chapter 5, Figures 7–9 illustrated the thermodynamic binding behavior of each metal ion from this investigation with the antioxidant GSH.

For the Cu(II) metal ion, the raw isotherm indicates that some sort of metal interaction is occurring with the GSH since the isotherm exothermic heat spike decreases significantly after fourth titrant injection before eventually tapering out for the remainder of the experiment. The Fe(II) metal ion isotherm from Figure 8 provides strong evidence supporting the notion that metal coordination is not occurring between the iron and the glutathione. Indication of this behavior is clearly seen in the raw isotherm that displays full peak heat spikes over the entire experimental run with no diminution to indicate metal binding had occurred between the metal titrant and antioxidant titrand.

In Figure 9 involving the Cu(I) metal ion and GSH, strong evidence is shown supporting the possibility of metal coordination. The raw isotherm data displays the tell-tale curve of an exothermic binding event. The high degree of fit of the binding model as well as the small standard deviations associated with the thermodynamic parameters is also indicative of a metal coordination event occurring. Investigations are ongoing since these preliminary results are promising.

7. CONCLUSIONS & FUTURE WORKS

Both the reduced form of glutathione (GSH) and dimethyl sulfoxide (DMSO) reduce the metal-mediated radical-induced oxidative DNA damage in reactions involving Cu(II), Fe(II), and Cu(I) with H_2O_2. While previous work had determined that DMSO achieved this effect through a radical scavenging scheme, the exact mechanism by which the sulfur based antioxidant GSH ameliorated the effects of radical-induced oxidative DNA damage has yet to be clearly elucidated. This study sought to address the question of which specific mechanism GSH used to mitigate the damaging effects of ROS – whether it is through via ROS scavenging, DNA adduction, or metal coordination.

The GSH concentration study demonstrates that an increased amount of the antioxidant leads to a direct decrease in the radical-induced site-specific DNA damage marker 8-OH-dG. The oxidative damage marker experiments involving GSH suggest that the antioxidant has roughly comparable detoxifying effects against metal-mediated oxidative DNA damage involving Cu(II), Fe(II), and Cu(I). However, in the chromatographic studies involving both GSH and DMSO, the Fe(II) metal ion tended to generate the least amount of the radical-induced 8-OH-dG damage marker. This effect correlates with the Fe(II) generating the largest amount of the non-radical induced dA *N*-1 oxide marker. Such a consistent result could be a result of differential metal-sulfur binding interactions, metal-DNA binding or a combination thereof. The 8-OH-dG levels in the Fe(II) trials may also be affected by the air oxidation that Fe(II) undergoes to Fe(III).

DCF-DA fluorescence studies suggest that the DMSO has comparable ROS reduction capabilities for the Cu(II), Fe(II), and Cu(I) metal systems. For the GSH experiments the DCF fluorescence supported the results for the Cu(II) and Cu(I) trials. However, the Fe(II) metal system actually exhibited an increase in ROS production when GSH was being used. These results suggest

that inorganic selenium compounds [6] may not be the only members of the chalcogen family that exhibit concentration-dependent anti- and pro-oxidant capabilities in the presence of redox-active metal ions.

The results from the ITC metal-GSH binding studies provide strong evidence that metal binding is not the mechanism of operation for the Fe(II) metal ion. However, the results for the Cu(II) trials suggest that some interaction may be occurring between the metal and the GSH. The Cu(I) trials provide the strongest evidence for metal coordination between the Cu(I) and GSH as a means of detoxifying the damaging effects of oxidative DNA damage.

The concentrations of the metals, DMSO, and H_2O_2 were not strictly indicative of physiological concentrations but they were optimized to provide a reasonably quantitative method of measuring the damaging effects of metal-mediated oxidative DNA damage. However, these species in conjunction with the GSH (which was investigated at a biologically relevant concentration) do help start to establish a more concise picture of the pro- and/or antioxidant capabilities of sulfur compounds by investigating how GSH behaves when compared against a known free radical scavenger in a battery of DNA damage marker and metal coordination studies.

The trends from Tables 5–7 do not exactly indicate that GSH behaves in a similar enough manner to DMSO to be considered a free radical scavenger. The marked differences in GSH and DMSO raise a few questions as to what differences can be expected between metal coordinating and radical scavenging antioxidants. These and other questions raised by the results from oxidative damage marker and fluorescent studies will likely be the focus of future studies involving the sulfur-based antioxidant GSH and the metal ions investigated in this study. In conclusion, the results from these experiments exploring metal-mediated oxidative DNA damage serve as a

starting point for establishing the basic science needed to help develop therapies for ailments that arise because of oxidative DNA damage.

The results from the present study did provide strong evidence supporting that the sulfur-based antioxidant, reduced glutathione or GSH, may be able to mitigate the toxic effects of Cu(I)-initiated oxidative DNA damage via metal coordination. Yet, due to the scope of the present work, a few limitations arose that would need to be addressed in future works before more conclusive determination can be drawn.

One major limitation that would need to be addressed in future works is the development of a method to determine the quantity of the Cu(II) that reduced to the Cu(I) oxidation state. This issue occurred when running the HPLC oxidative damage marker studies since copper compounds are known to undergo very efficient redox cycling [68] and thus make determination of the metal ion's oxidation state difficult.

Due to the inefficiencies in the chromatographic method, slight side-oxidation of the normal DNA bases may occur [46]. Such inefficiencies may add errors to the retention times of the peak fractions for the DNA strands. Issues such as these may be resolved with the use of the chromatographic in conjunction with DNA repair glycosylases with the Comet assay [46]. These techniques would yield a more precise way of monitoring the oxidized bases of interest, such as the guanine base in the 8-OH-dG marker.

The use of spin-trapping experiments via electron paramagnetic resonance (EPR) spectroscopy and various spin trapping agents would help identify and monitor the various reactive radical species being generated during the experiments [69]. Future studies could then be developed to investigate how the identity of the radical species plays into the amount of damage

that is seen. Such experiments would further confirm if the hydroxyl radical is truly being formed in the DCF-DA fluorescence studies.

To establish more quantitative base measurements of the radical scavenging mechanism of DMSO, an electron spin resonance (ESR) spin trapping-based multiple free-radical scavenging (MULTIS) experiment [70] can be performed. The experiment would provide baseline measurements for a known radical scavenger, such as DMSO, against different radical species such as hydroxyl radical, superoxide anion, and singlet oxygen. These values would then serve as targets that the GSH could possibly achieve if radical scavenging was truly its mechanism of operation.

The possibility of the antioxidant binding to the DNA to form some sort of adduct which in turn prevents the oxidation of the nucleobases, especially the guanine, is a method by which the antioxidant could detoxify the damaging effects of oxidative DNA damage. To confirm if this option is a viable mechanism, a high-throughput fluorescent intercalator displacement (HT-FID) assay with a high-resolution (HR) crystallographic method could be used [71]. This ethidium bromide assay would have varying degrees of fluorescent intensity to correspond to the possible binding event between the DNA and antioxidant.

LIST OF REFERENCES

[1] Podhorecka, M., Skladanowski, A. & Bozko, P. “H2AX Phosphorylation: Its Role in DNA Damage Response and Cancer Therapy”. *J. Nucleic Acids* **2011**(6): 1–9 (2011).

[2] Nouspikel, T. “So DNA repair really is that important?” *Cell. Mol. Life Sci.* **66**(6): 965–967 (2009).

[3] Battin, E. E. & Brumaghim, J. L. “Antioxidant activity of sulfur and selenium: A review of reactive oxygen species scavenging, glutathione peroxidase, and metal-binding antioxidant mechanisms”. *Cell Biochemistry and Biophysics* **55**(1): 1–23 (2009).

[4] Devasagayam, T. P. A. *et al.* “Free radicals and antioxidants in human health: current status and future prospects”. *J. Assoc. Physicians India* **52**: 794–804 (2004).

[5] Paz-Elizur, T., Brenner, D. E. & Livneh, Z. “Interrogating DNA repair in cancer risk assessment”. *Cancer Epidemiol. Biomarkers Prev.* **14**(7): 1585–1587 (2005).

[6] Lengauer, C., Kinzler, K. W. & Vogelstein, B. “Genetic instability in colorectal cancers”. *Nature* **386**(6625): 623–627 (1997).

[7] Zimmerman, M. T., Bayse, C. A., Ramoutar, R. R. & Brumaghim, J. L. “Sulfur and selenium antioxidants : Challenging radical scavenging mechanisms and developing structure – activity relationships based on metal binding”. *J. Inorg. Biochem.* **145**(1): 30–40 (2015).

[8] Hart, W. E., Marczak, S. P., Kneller, A. R., French, R. a. & Morris, D. L. “The abilities of selenium dioxide and selenite ion to coordinate DNA-bound metal ions and decrease oxidative DNA damage”. *J. Inorg. Biochem.* **125**: 1–8 (2013).

[9] Battin, E. E. & Brumaghim, J. L. “Metal specificity in DNA damage prevention by sulfur antioxidants”. *J. Inorg. Biochem.* **102**(12): 2036–2042 (2008).

[10] Weinberg, R. A. (2014). Cells deploy a variety of defenses to protect DNA molecules from attack by mutagens. In E. Zayatz (Ed.), *The Biology of Cancer* (2nd ed.), pp. 535–537. New York, NY: Garland Science, Taylor & Francis Group, LLC.

[11] Reese, J. B. *et al.* (2011). Membrane Structure and Function. In B. Wilbur (Ed.), *Campbell Biology* (9th ed.), pp. 125–127. San Francisco, CA: Pearson Benjamin Cummings.

[12] Marnett, L. J. “Lipid peroxidation-DNA damage by malondialdehyde”. *Mutat. Res.* **424**(1-2): 83–95 (1999).

[13] German, J. B. “Food processing and lipid oxidation”. *Adv. Exp. Med. Biol.* **459**: 23–50 (1999).

[14] Sies, H. “Oxidative stress: oxidants and antioxidants”. *Exp. Physiol.* **82**(2): 291–295 (1997).

[15] Jomova, K. & Valko, M. “Advances in metal-induced oxidative stress and human disease”. *Toxicology* **283**(2-3): 65–87 (2011).

[16] Vinceti, M. *et al.* “Selenium for preventing cancer”. *Cochrane database Syst. Rev.* **3,** CD005195 (2014).

[17] Valko, M. *et al.* “Free radicals and antioxidants in normal physiological functions and human disease”. *Int. J. Biochem. Cell Biol.* **39**(1): 44–84 (2007).

[18] Jiang, L. *et al.* “Efficacy of antioxidant vitamins and selenium supplement in prostate cancer prevention: a meta-analysis of randomized controlled trials”. *Nutr. Cancer* **62**(6): 719–727 (2010).

[19] Shekelle, P. G. *et al.* “Effect of supplemental vitamin E for the prevention and treatment of cardiovascular disease”. *J. Gen. Intern. Med.* **19**(4): 380–389 (2004).

[20] Knight, J. A. “Free radicals: their history and current status in aging and disease”. *Ann. Clin. Lab. Sci.* **28**(6): 331–346 (1998).

[21] Davies, K. J. “Oxidative stress: the paradox of aerobic life”. *Biochem. Soc. Symp.* **61**: 1–31 (1995).

[22] Schulz, J. B., Lindenau, J., Seyfried, J. & Dichgans, J. “Glutathione, oxidative stress and neurodegeneration”. *Eur. J. Biochem.* **267**: 4904–4911 (2000).

[23] Barbusinski, K. “Fenton reaction - Controversy concerning the chemistry”. *Ecol. Chem. Eng. S/Chemia i in·zynieria Ekol. S* **16**(3): 347–358 (2009).

[24] Valko, M., Rhodes, C. J., Moncol, J., Izakovic, M. & Mazur, M. “Free radicals, metals and antioxidants in oxidative stress-induced cancer”. *Chem. Biol. Interact.* **160**(1): 1–40 (2006).

[25] Weimann, A., Belling, D. & Poulsen, H. E. “Quantification of 8-oxo-guanine and guanine as the nucleobase, nucleoside and deoxynucleoside forms in human urine by high-performance liquid chromatography-electrospray tandem mass spectrometry”. *Nucleic Acids Res.* **30**(2): E7 (2002).

[26] Cotran, R., Kumar, V., & Collins, T. (1999). *Robbins Pathologic Basis of Disease* (6th ed.). Philadelphia, PA: W.B. Saunders.

[27] Anastassopoulou, J. “Metal-DNA interactions”. *J. Mol. Struct.* **651-653,** 19–26 (2003).

[28] Lippert, B. “Multiplicity of metal ion binding patterns to nucleobases”. *Coord. Chem. Rev.* **200-202,** 487–516 (2000).

[29] Rosemeyer, H. “The chemodiversity of purine as a constituent of natural products”. *Chem. Biodivers.* **1**(3): 361–401 (2004).

[30] “The DNA Double Helix”. Digital Image. *Boundless Biology*. Boundless, 21 Jul 2015. Web. 29 Jul 2015.

<https://www.boundless.com/biology/textbooks/boundless-biology-textbook/biological-macromolecules-3/nucleic-acids-57/the-dna-double-helix-307-11440/>.

[31] Tereshko, V. *et al.* “Detection of alkali metal ions in DNA crystals using state-of-the-art X-ray diffraction experiments”. *Nucleic Acids Res.* **29**(5): 1208–1215 (2001).

[32] Boysen, G., Pachkowski, B. F., Nakamura, J. & Swenberg, J. A. “The formation and biological significance of N7-guanine adducts”. *Mutat. Res.* **678**(2): 76–94 (2009).

[33] Ameyar, M., Wisniewska, M. & Weitzman, J. B. “A role for AP-1 in apoptosis: the case for and against”. *Biochimie* **85**(8): 747–752 (2003).

[34] Gilmore, T. D. “Introduction to NF-kappaB: players, pathways, perspectives”. *Oncogene* **25**(51): 6680–6684 (2006).

[35] Perkins, N. D. Integrating cell-signaling pathways with NF-kappaB and IKK function. *Nat. Rev. Mol. Cell Biol.* **8**(1): 49–62 (2007).

[36] Brasier, A. R. “The NF-kappaB regulatory network”. *Cardiovasc. Toxicol.* **6**(2): 111–130 (2006).

[37] Gajewski, E., Rao, G., Nackerdien, Z. & Dizdaroglu, M. “Modification of DNA bases in mammalian chromatin by radiation-generated free radicals”. *Biochemistry* **29**(34): 7876–7882 (1990).

[38] Ames, B. N. & Gold, L. S. “Endogenous mutagens and the causes of aging and cancer”. *Mutat. Res.* **250**(1-2): 3–16 (1991).

[39] Taddei, F. *et al.* “Counteraction by MutT protein of transcriptional errors caused by oxidative damage”. *Science* **278**(5335): 128–130 (1997).

[40] Hepel, M., Stobiecka, M., Peachey, J. & Miller, J. “Intervention of glutathione in pre-mutagenic catechol-mediated DNA damage in the presence of copper(II) ions”. *Mutat. Res.* **735**(1-2): 1–11 (2012).

[41] Shibutani, S., Takeshita, M. & Grollman, A. P. “Insertion of specific bases during DNA synthesis past the oxidation-damaged base 8-oxodG”. *Nature* **349**(6308): 431–434 (1991).

[42] De Souza-Pinto, N. C. *et al.* “Repair of 8-oxodeoxyguanosine lesions in mitochondrial DNA depends on the oxoguanine DNA glycosylase (OGG1) gene and 8-oxoguanine accumulates in the mitochondrial DNA of OGG1-defective mice”. *Cancer Res.* **61**(14): 5378–5381 (2001).

[43] Mouret, J. F., Polverelli, M., Sarrazini, F. & Cadet, J. “Ionic and radical oxidations of DNA by hydrogen peroxide”. *Chem. Biol. Interact.* **77**(2): 187–201 (1991).

[44] Tice, R. R. *et al.* Single cell gel/comet assay: guidelines for in vitro and in vivo genetic toxicology testing. *Environ. Mol. Mutagen.* **35**(3): 206–221 (2000).

[45] Park, E. M. *et al.* “Assay of excised oxidative DNA lesions: isolation of 8-oxoguanine and its nucleoside derivatives from biological fluids with a monoclonal antibody column”. *Proc. Natl. Acad. Sci. U. S. A.* **89**(8): 3375–3379 (1992).

[46] Cadet, J. *et al.* “Assessment of oxidative base damage to isolated and cellular DNA by HPLC-MS/MS measurement”. *Free Radic. Biol. Med.* **33**(4): 441–449 (2002).

[47] Wuguo, D., Xingwang, F. & Jilan, W. “Flavonoids function as antioxidants: By scavenging reactive oxygen species or by chelating iron?” *Radiat. Phys. Chem.* **50**(3): 271–276 (1997).

[48] Masella, R., Di Benedetto, R., Varì, R., Filesi, C. & Giovannini, C. “Novel mechanisms of natural antioxidant compounds in biological systems: involvement of glutathione and glutathione-related enzymes”. *J. Nutr. Biochem.* **16**(10): 577–586 (2005).

[49] Jani, N., Ziogas, J., Angus, J. A. & Wright, C. E. “Exogenous glutathione is essential in the testing of antioxidant capacity using radical-induced haemolysis”. *J. Pharmacol. Toxicol. Methods* **65**(3): 142–146 (2012).

[50] Gérard-Monnier, D. & Chaudiere, J. “Metabolism and antioxidant function of glutathione”. *Pathol. Biol. (Paris).* **44**(1): 77–85 (1996).

[51] Lu, S.C. “Regulation of glutathione synthesis”. *Mol. Aspects Med.* **30**(1–2): 42–59 (2009).

[52] Glutathione structure. Digital Image. InTech, n.d. Web. 14 Jun 2015. <http://www.intechopen.com/source/html/17260/media/image5.png>.

[53] Li, J., Zhang, D., Jefferson, P. A., Ward, K. M. & Ayene, I. S. “A bioactive probe for glutathione-dependent antioxidant capacity in breast cancer patients: implications

in measuring biological effects of arsenic compounds". *J. Pharmacol. Toxicol. Methods* **69**(1): 39–48 (2014).

[54] Mugesh, G. & Singh, H. B. "Synthetic organoselenium compounds as antioxidants: glutathione peroxidase activity". *Chem. Soc. Rev.* **29**(5): 347–357 (2000).

[55] Collins, C. A. *et al.* "Towards multifunctional antioxidants: synthesis, electrochemistry, in vitro and cell culture evaluation of compounds with ligand/catalytic properties". *Org. Biomol. Chem.* **3**(8): 1541–1546 (2005).

[56] Lin, S., Tsai, S., Lee, S. & Wu, S. "Effects of Storage Time and Temperature on the Stability of Glutathione in Deproteinized Blood Sample". *J. Food Drug Anal.* **14**(2): 141–146 (2006).

[57] Smith, C. V, Jones, D. P., Guenthner, T. M., Lash, L. H. & Lauterburg, B. H. "Compartmentation of glutathione: implications for the study of toxicity and disease". *Toxicol. Appl. Pharmacol.* **140**(1): 1–12 (1996).

[58] Novak, K. M., ed. (2002). *Drug Facts and Comparisons* (56th ed.), p. 619. St. Louis, Missouri: Wolters Kluwer Health.

[59] Sanmartín-Suárez, C., Soto-Otero, R., Sánchez-Sellero, I. & Méndez-Álvarez, E. "Antioxidant properties of dimethyl sulfoxide and its viability as a solvent in the evaluation of neuroprotective antioxidants". *J. Pharmacol. Toxicol. Methods* **63**(2): 209–215 (2011).

[60] Tam, S. P., Zhang, X., Cuthbert, C., Wang, Z. & Ellis, T. "Effects of dimethyl sulfoxide on apolipoprotein A-I in the human hepatoma cell line, HepG2". *J. Lipid Res.* **38**(10): 2090–2102 (1997).

[61] Kwak, G.-H., Choi, S. H. & Kim, H.-Y. "Dimethyl sulfoxide elevates hydrogen peroxide-mediated cell death in Saccharomyces cerevisiae by inhibiting the antioxidant function of methionine sulfoxide reductase A". *BMB Rep.* **43**(9): 622–628 (2010).

[62] Depraetere, S., Vanhaesebroeck, B., Fiers, W., Willems, J. & Joniau, M. "Polar agents with differentiation inducing capacity potentiate tumor necrosis factor-mediated cytotoxicity in human myeloid cell lines". *J. Leukoc. Biol.* **57**(1): 141–151 (1995).

[63] Hsu, K. H. & Friedman, H. "Dimethyl sulfoxide-induced transglutaminase activity in murine-derived Friend erythroleukemia cells". *J. Natl. Cancer Inst.* **70**(5): 965–969 (1983).

[64] Pierce, M. M., Raman, C. S. & Nall, B. T. "Isothermal titration calorimetry of protein-protein interactions". *Methods* **19**(2): 213–221 (1999).

[65] Brown, R. K., Brandts, J. M., Peters, R. O. & Peters, W. B. (2009). ITC-derived binding constants: Using microgram quantities of protein. *Label-Free Biosensors* (pp. 223–250). Cambridge, UK: Cambridge University Press.

[66] Freyer, M. W. & Lewis, E. A. "Isothermal Titration Calorimetry: Experimental Design, Data Analysis, and Probing Macromolecule/Ligand Binding and Kinetic Interactions". *Methods Cell Biol.* **84**(7): 79–113 (2008).

[67] *TA Instruments NanoAnalyze™ Software Getting Started Guide*. TA Instruments. 2014.

[68] Morris, D. L. "DNA-bound metal ions: recent developments". *Biomol. Concepts* **5**(5): 397–407 (2014).

[69] Bobeničová, M., Valko, M., Brezová, V. & Dvoranová, D. "UVA generated free radicals in irinotecan (CPT-11) in the presence of copper ions". *J. Photochem. Photobiol. A Chem.* **290**(1): 125–138 (2014).

[70] Kamogawa, E. & Sueishi, Y. "A multiple free-radical scavenging (MULTIS) study on the antioxidant capacity of a neuroprotective drug, edaravone as compared with uric acid, glutathione, and trolox". *Bioorganic Med. Chem. Lett.* **24**(5): 1376–1379 (2014).

[71] Goodwin, K. D. *et al.* "A high-throughput, high-resolution strategy for the study of site-selective DNA binding agents: analysis of a 'highly twisted' benzimidazole-diamidine". *J. Am. Chem. Soc.* **128**(24): 7846–7854 (2006).